Supporting Information - Synthesis and analysis of the anticancer activity of platinum(II) complexes incorporating dipyridoquinoxaline variants

*Benjamin J. Pages, Feng Li, Paul Wormell, Dale L. Ang, Jack K. Clegg, Cameron J. Kepert, Lawson K. Spare, Supawich Danchaiwijit, Janice R. Aldrich-Wright.**

Table of Contents

Section S1 – Sep-Pak Column Method Development

As stated in the main text, the first 10 mL of Sep-Pak® eluent were discarded in order to remove impurities with quicker elution speeds than the final product. The discovery that some impurities eluted from the column before each final product was made when ^{1}H NMR spectra were obtained for four separate fractions that were collected from the elution of complex **1** through a Sep-Pak®. The ^{1}H-^{195}Pt HMQC spectrum of the first fraction was also obtained (Figure S1.1).

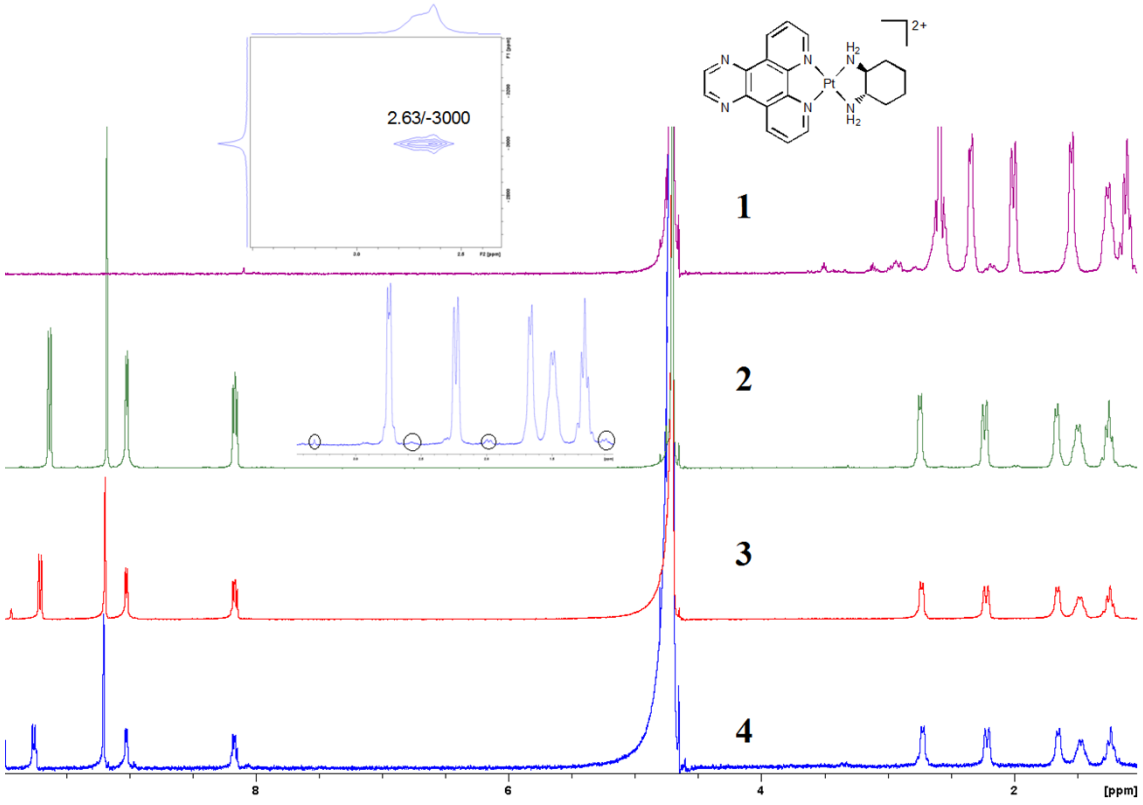

Figure S1.1. ^{1}H NMR spectra of the complex **1** fractions obtained from the Sep-Pak®. Inset: the ^{195}H/^{195}Pt spectrum of the first fraction (above) and the zoomed in aliphatic region of fraction 2 (below). Impurities of the second fraction are circled. The peaks close to the solvent resonances are due to D_2O impurities.

The ^{1}H NMR spectrum of the first fraction revealed only peaks that represented dach and no resonances corresponding to dpq; this suggested that unreacted [Pt(*SS*-dach)Cl_2] had eluted from the column before complex **1**. In the ^{1}H-^{195}Pt HMQC spectrum, the presence of a platinum species coupled to a proton in the aliphatic region suggests the presence of [Pt(*SS*-dach)Cl_2]. The Pt chemical shift of -3000 ppm is not consistent with the reported shift of -3282 ppm for [Pt(*SS*-dach)Cl_2];[1] however, it is possible that hydrolysis in D_2O could have

produced [Pt(*SS*-dach)(D_2O)Cl], similarly to the hydrolysis of cisplatin *in vivo*.[2] This would result in a different ^{195}Pt chemical shift, and so unreacted [Pt(*SS*-dach)Cl_2] is therefore likely to be this impurity. This is significant as previous Sep-Pak® methodologies did not involve the discarding of any initial eluted solvent.[3] The ^{1}H NMR spectrum of the second fraction showed peaks corresponding to both complex **1** and the impurity in the first fraction, indicating that an overlap of elution had occurred. The ^{1}H NMR spectra of the 3rd and 4th fractions subsequently showed complex **1** only, with impurities at an acceptably low level (< 2%). Due to these results, subsequent Sep-Pak® purifications followed the methodology described in the main text in which the first 10 mL to elute was discarded. The success of this methodology is seen in the ^{1}H NMR spectra of collected fractions of complex **2** (Figure S1.2). The collection of a larger volume in the first fraction resulted in some loss of final product, but ensured that subsequent fractions were acceptably pure.

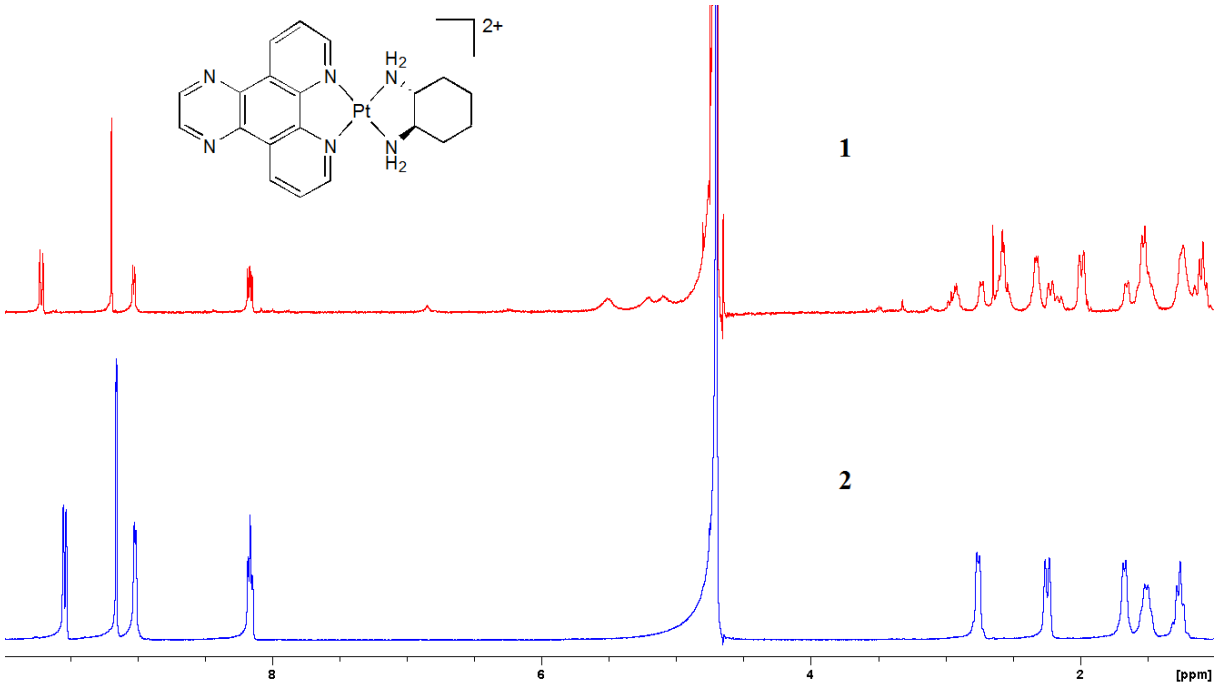

Figure S1.2. ^{1}H NMR spectra of the first two complex **2** fractions obtained from the Sep-Pak® elution. The third and fourth fractions showed the same level of purity as the second.

Section S2 – Characterisation Data

S2.1. UV Data

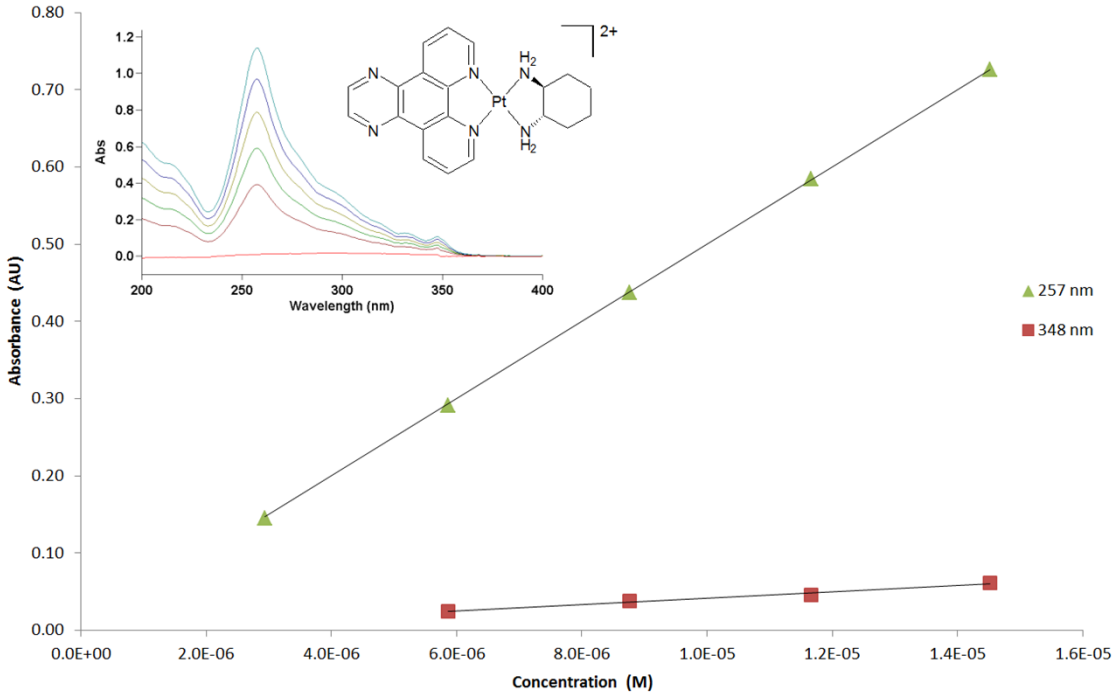

Figure S2.1.1. Standard absorbance plot of complex **1**, obtained from the titration of the complex into water. Inset: the absorbance spectra recorded over the course of titrations.

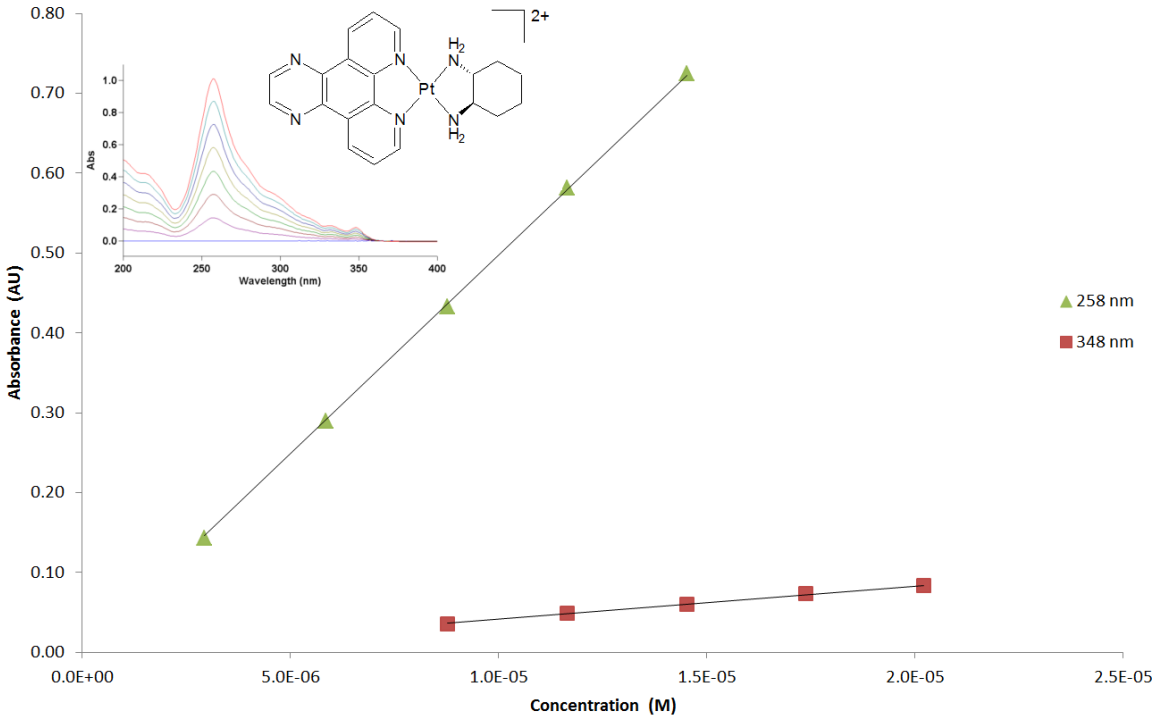

Figure S2.1.2. Standard absorbance plot of complex **2**, obtained from the titration of the complex into water. Inset: the absorbance spectra recorded over the course of titrations.

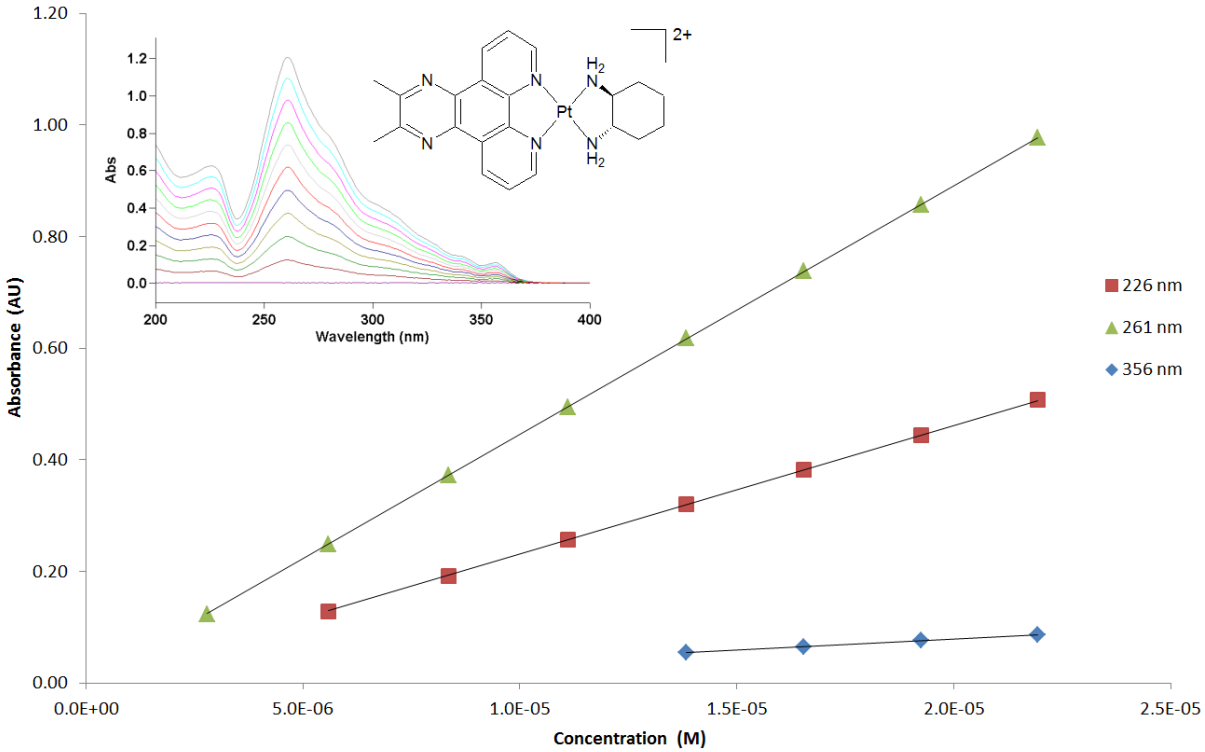

Figure S2.1.3. Standard absorbance plot of complex **3**, obtained from the titration of the complex into water. Inset: the absorbance spectra recorded over the course of titrations.

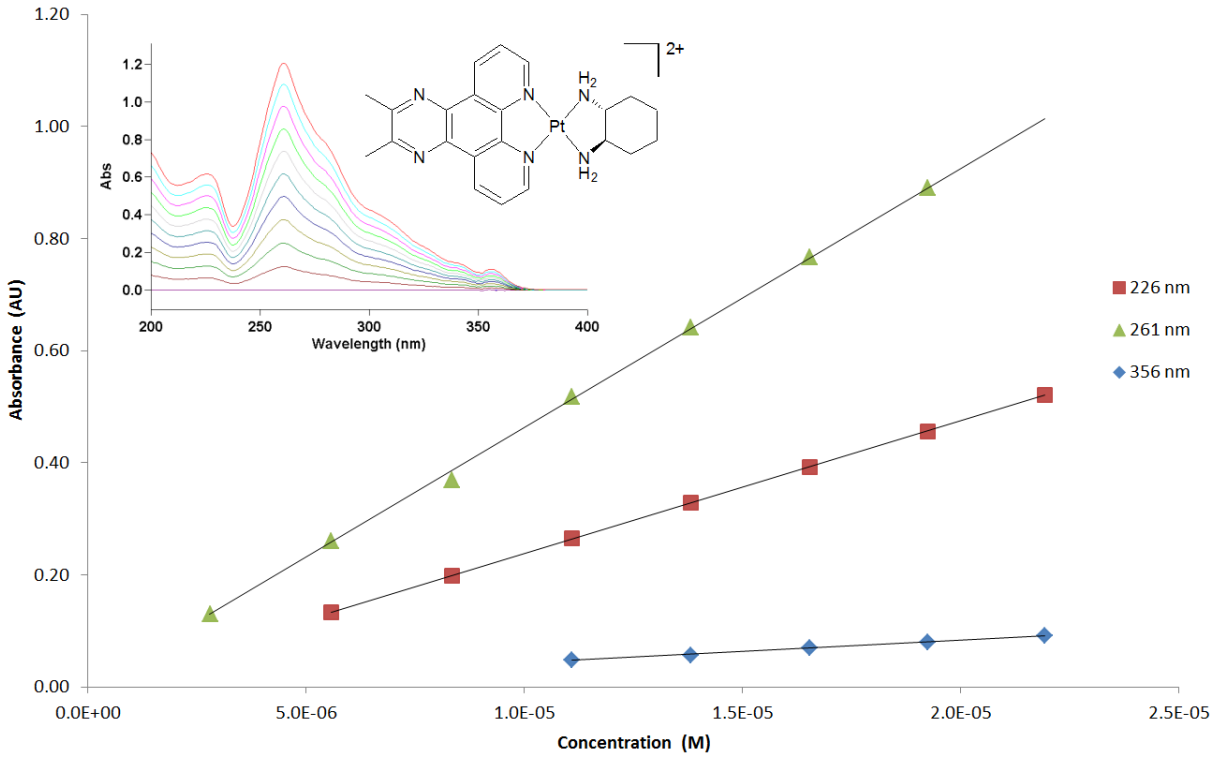

Figure S2.1.4. Standard absorbance plot of complex **4**, obtained from the titration of the complex into water. Inset: the absorbance spectra recorded over the course of titrations.

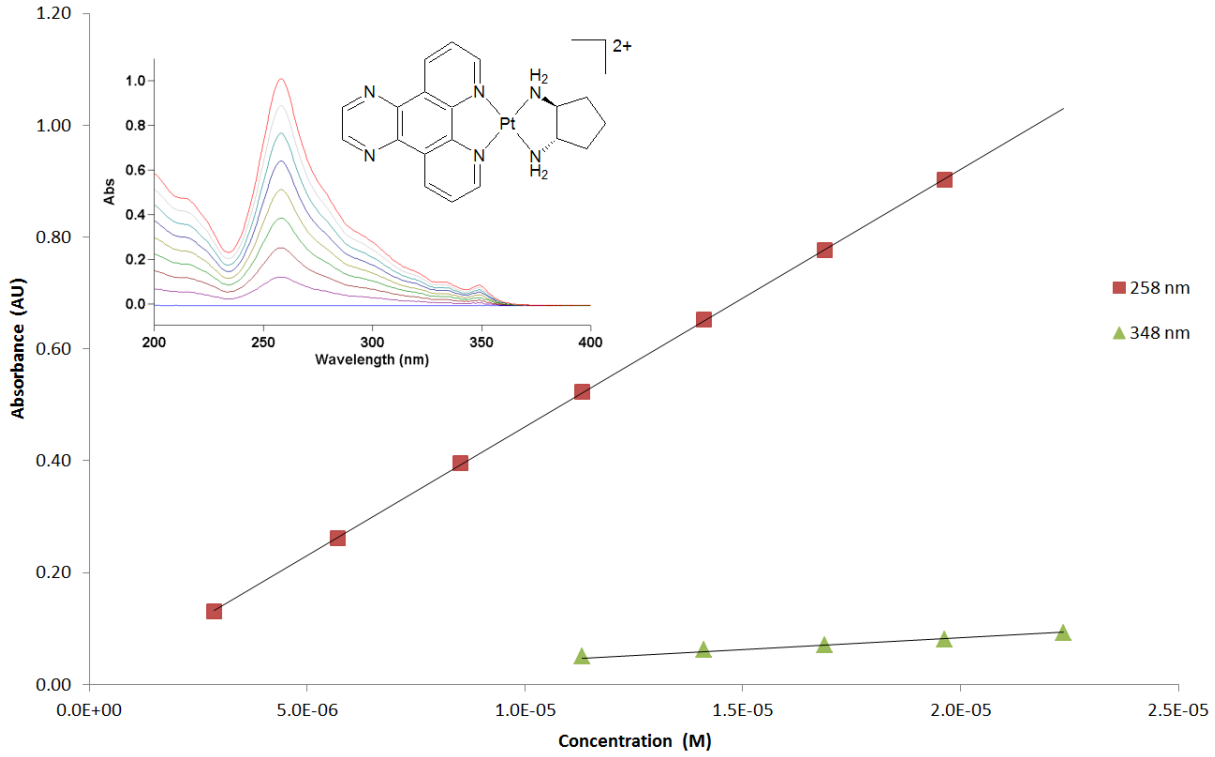

Figure S2.1.5. Standard absorbance plot of complex **5**, obtained from the titration of the complex into water. Inset: the absorbance spectra recorded over the course of titrations.

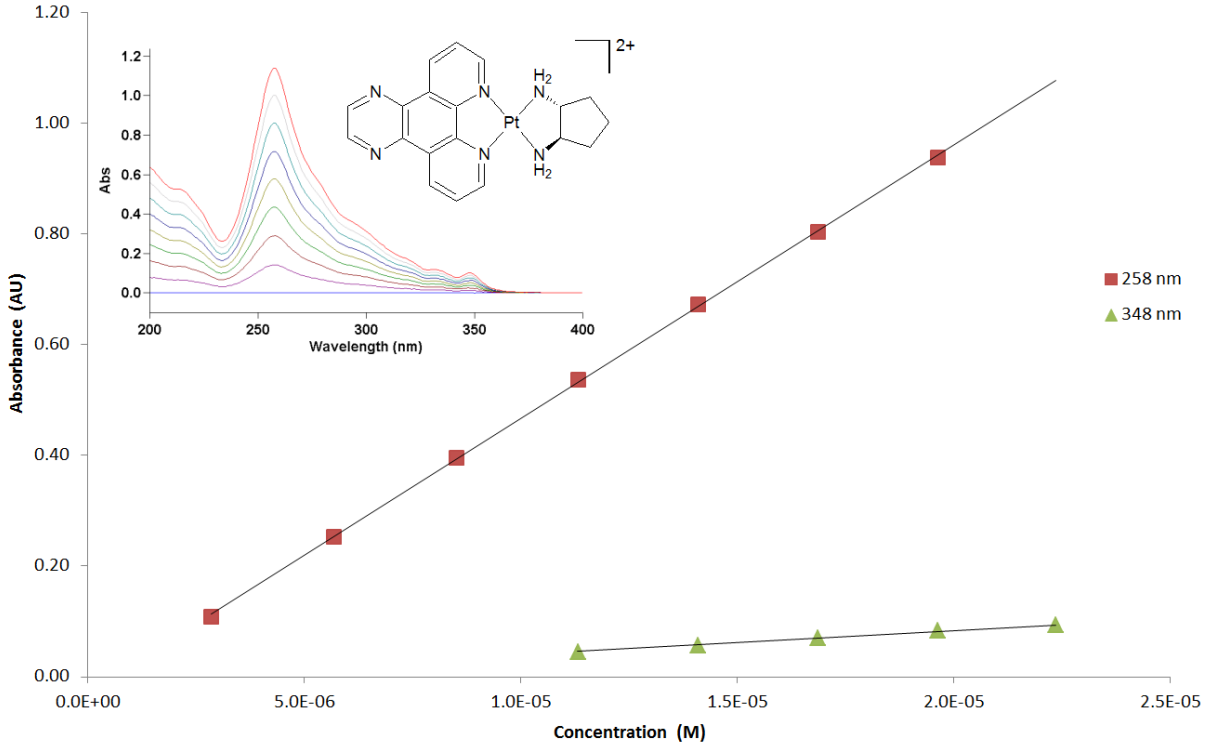

Figure S2.1.6. Standard absorbance plot of complex **6**, obtained from the titration of the complex into water. Inset: the absorbance spectra recorded over the course of titrations.

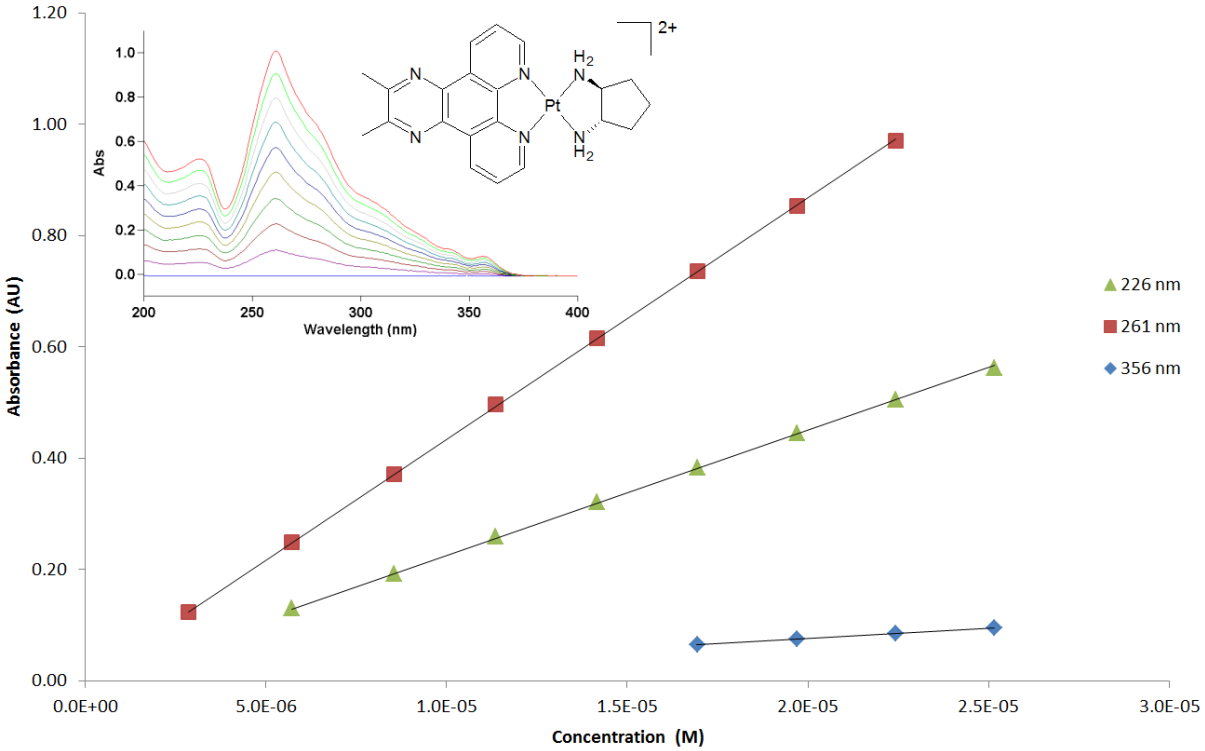

Figure S2.1.7. Standard absorbance plot of complex **7**, obtained from the titration of the complex into water. Inset: the absorbance spectra recorded over the course of titrations.

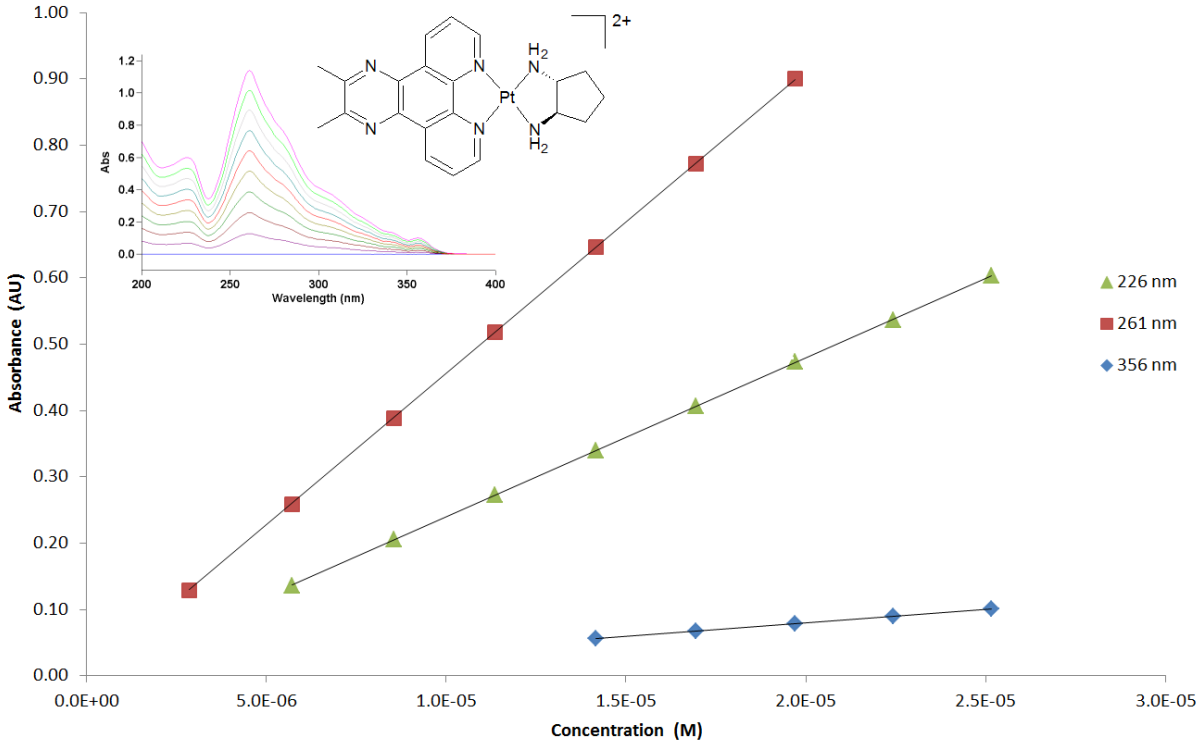

Figure S2.1.8. Standard absorbance plot of complex **8**, obtained from the titration of the complex into water. Inset: the absorbance spectra recorded over the course of titrations.

S2.2. CD Spectra

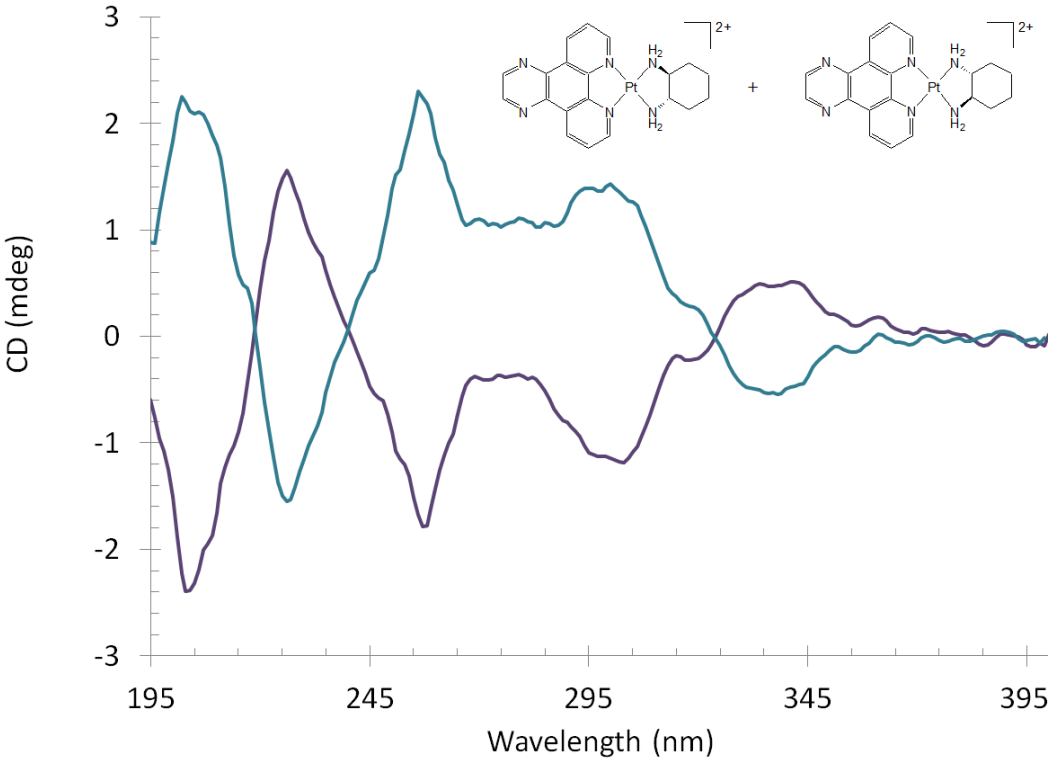

Figure S2.2.1. The CD spectra of complexes **1** (purple) and **2** (blue).

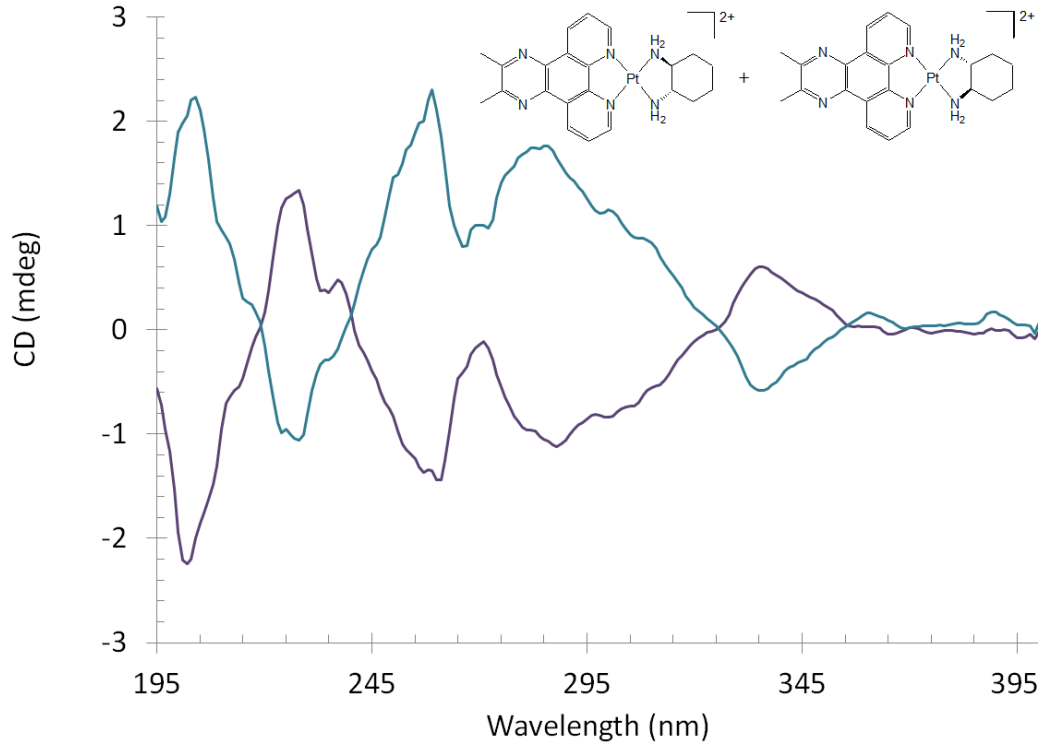

Figure S2.2.2. The CD spectra of complexes **3** (purple) and 4 (blue).

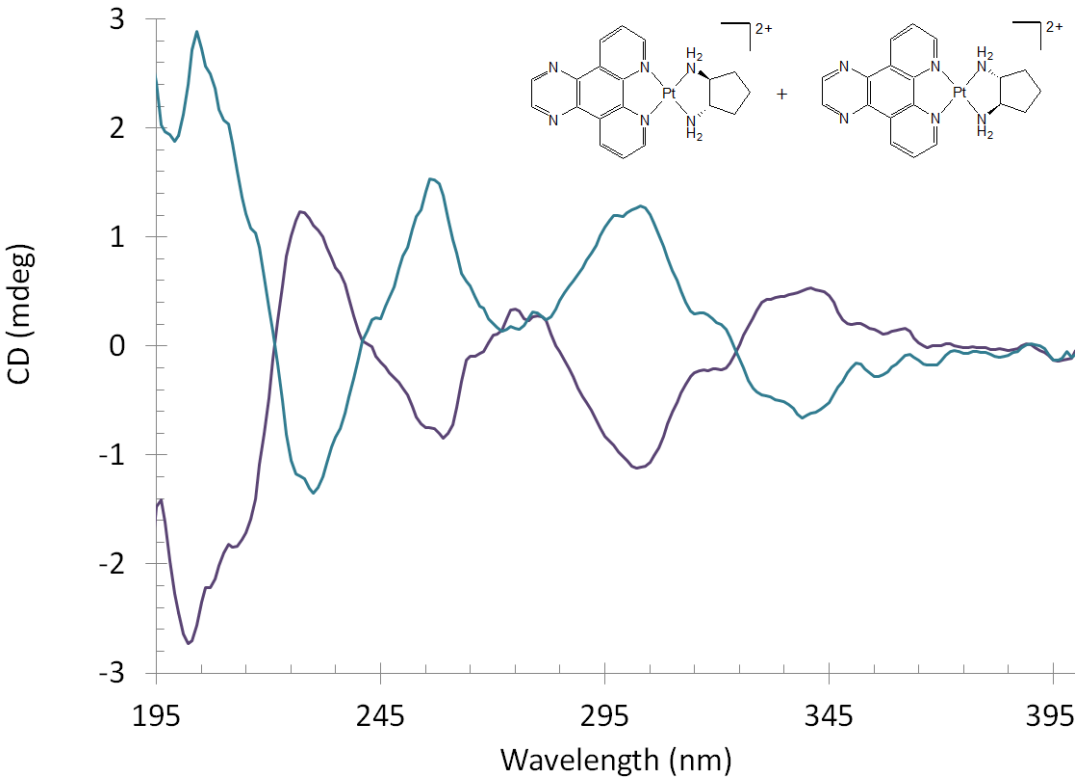

Figure S2.2.3. The CD spectra of complexes **5** (purple) and **6** (blue).

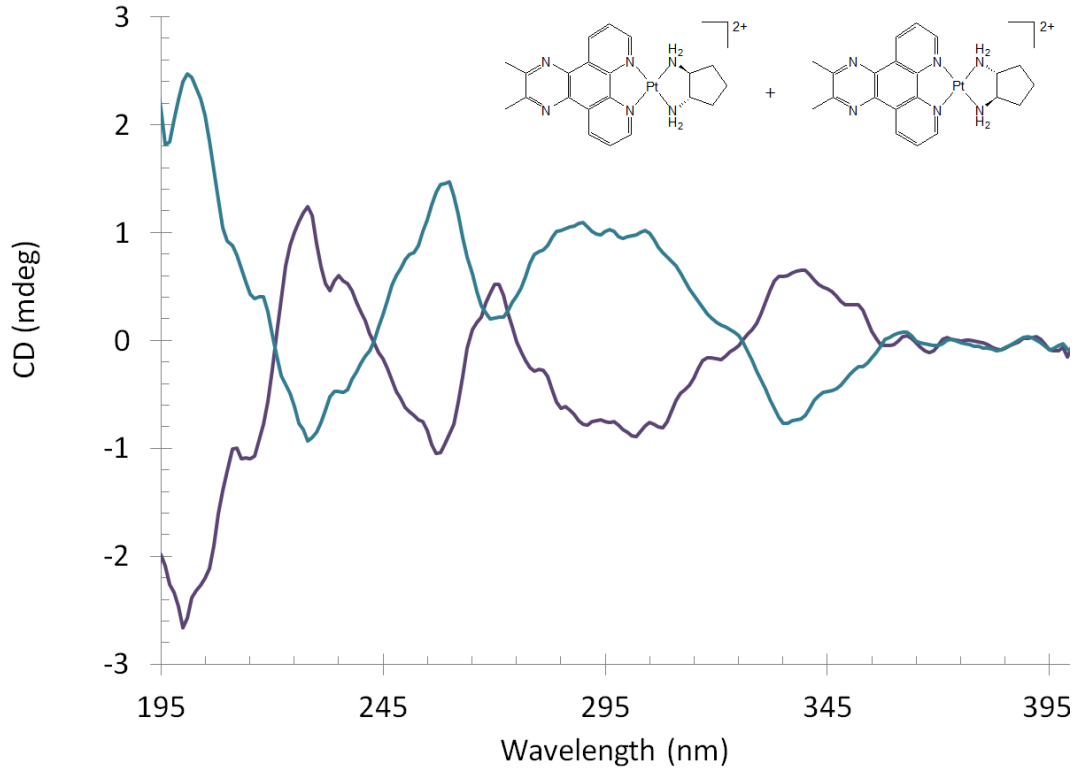

Figure S2.2.4. The CD spectra of complexes **7** (purple) and **8** (blue).

S2.3. ^{1}H NMR Spectra

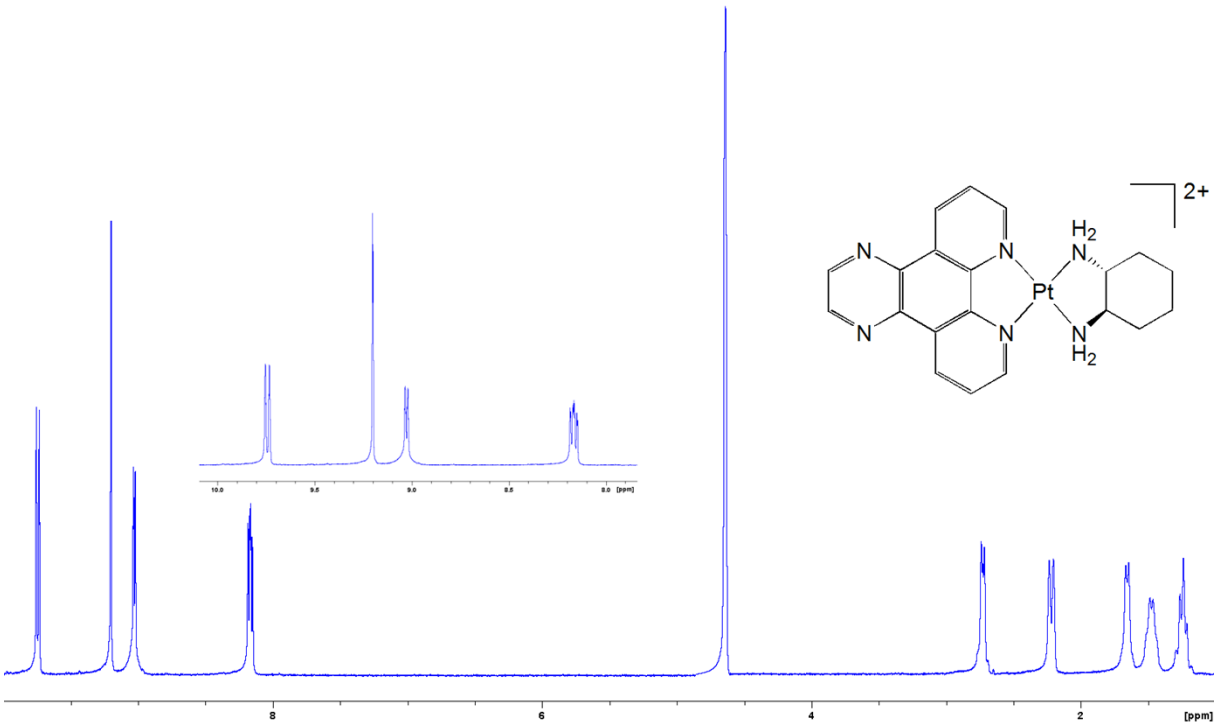

Figure S2.3.1. The ^{1}H NMR spectrum of complex **2** in D_2O.

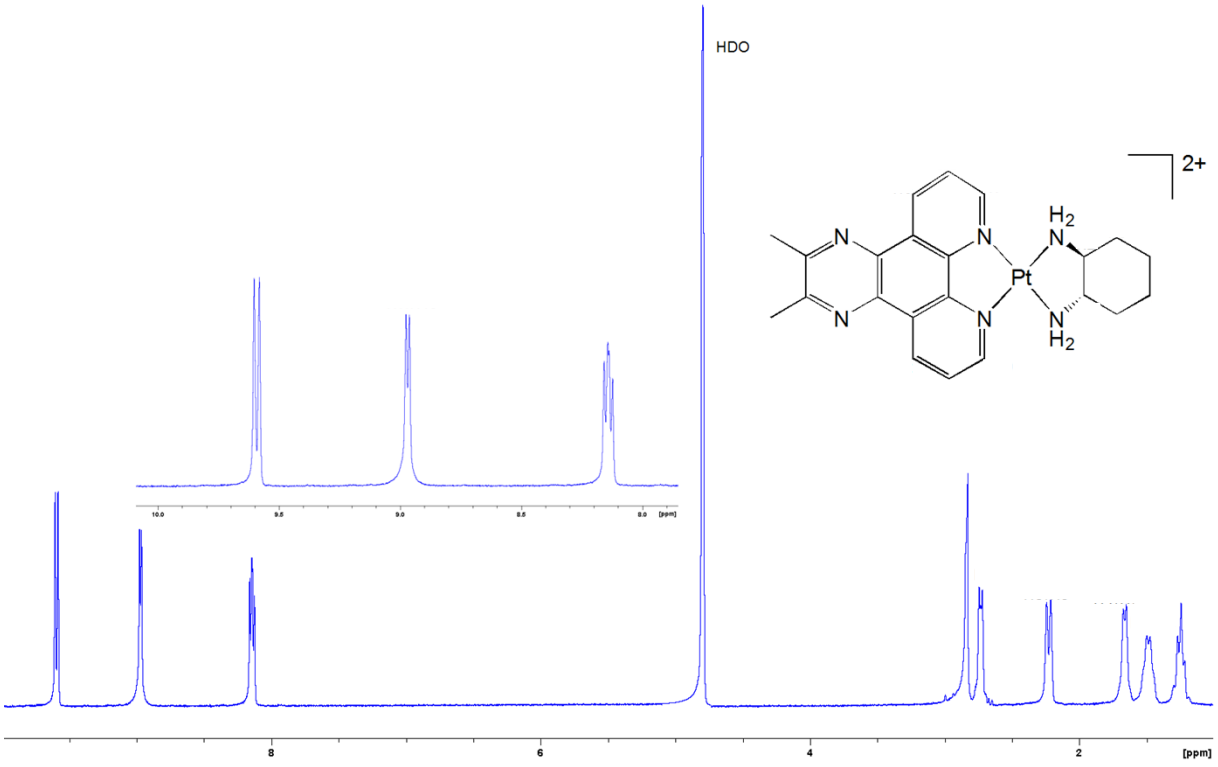

Figure S2.3.2. The ^{1}H NMR spectrum of complex **3** in D_2O

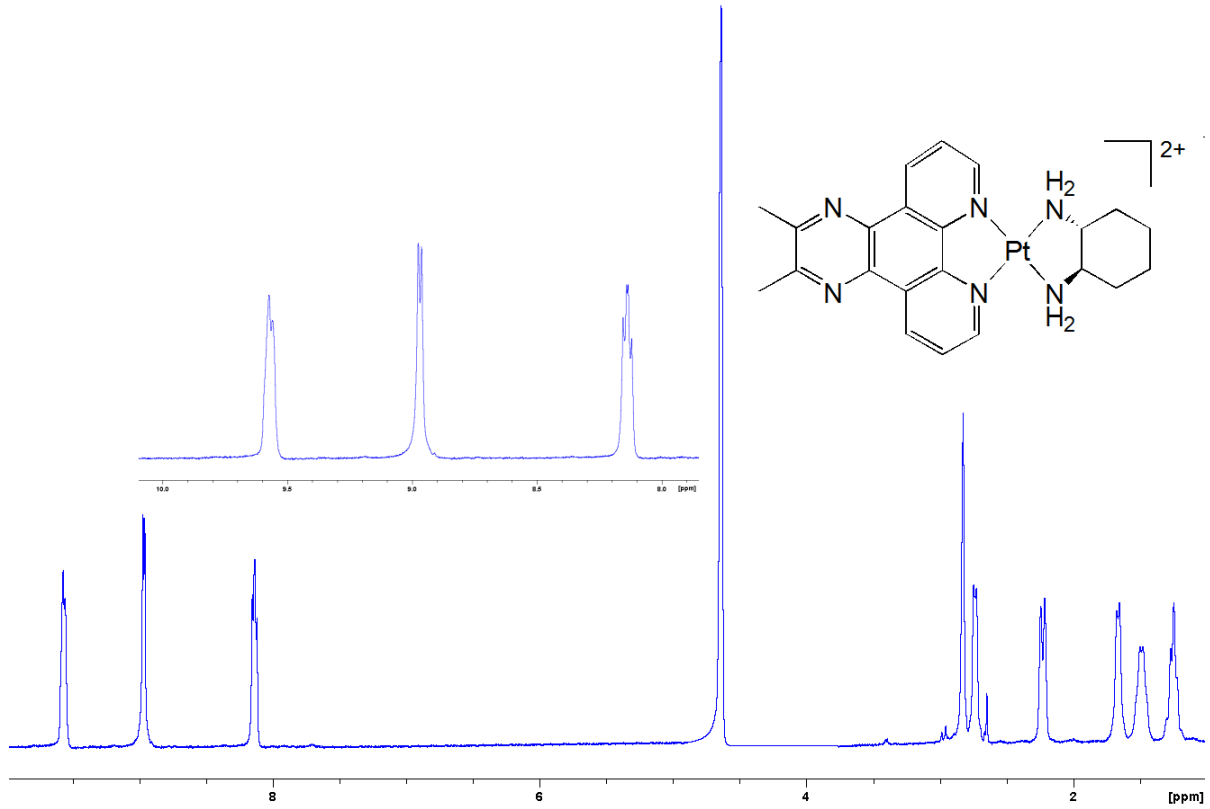

Figure S2.3.3. The ^{1}H NMR spectrum of complex **4** in D_2O.

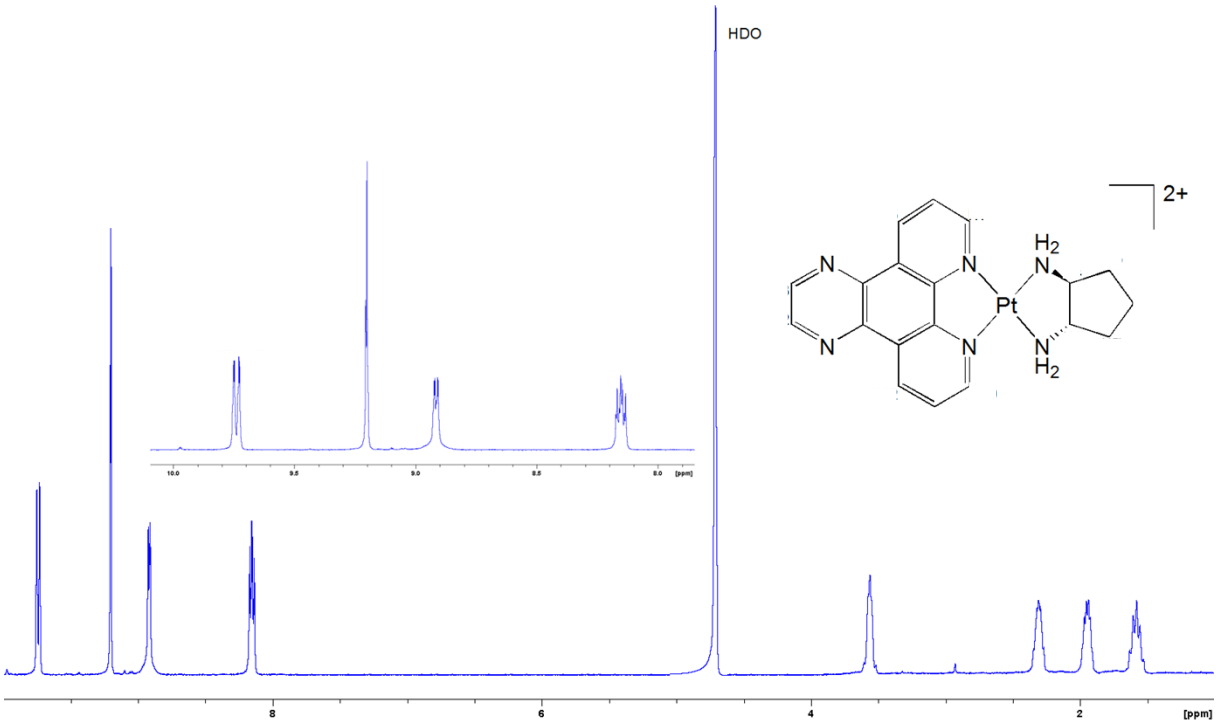

Figure S2.3.4. The ^{1}H NMR spectrum of complex **5** in D_2O.

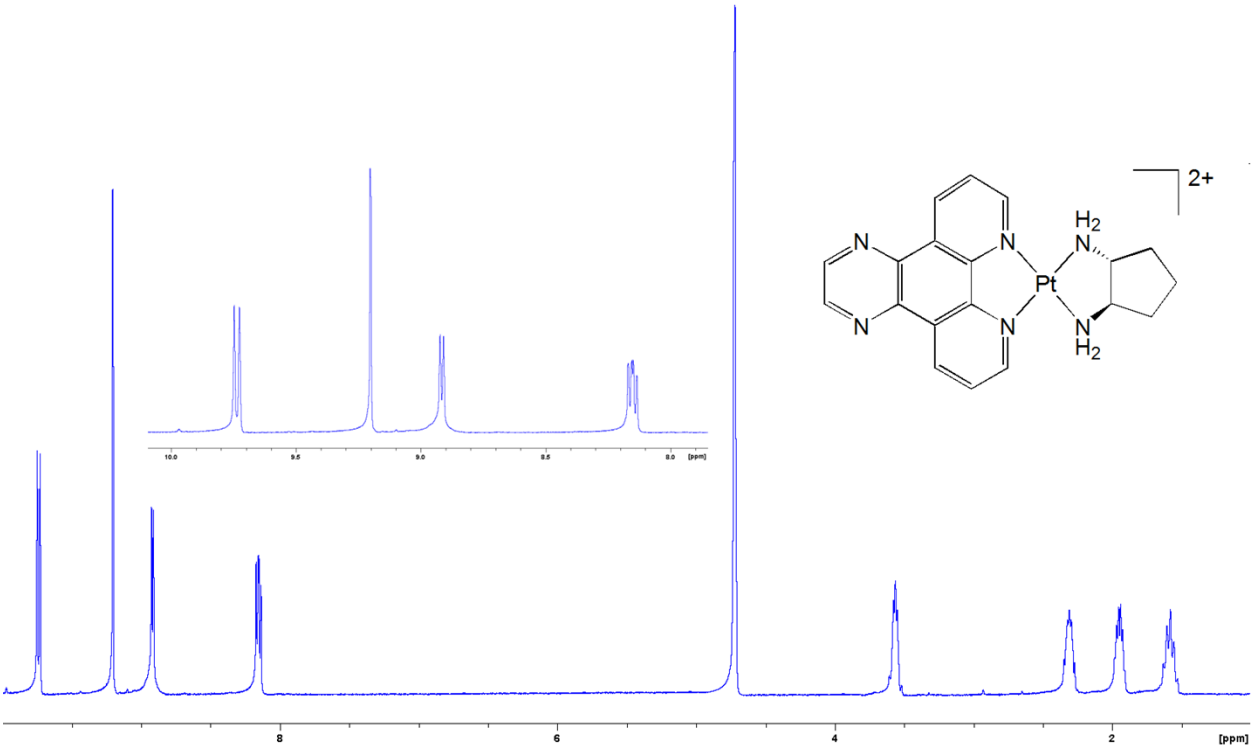

Figure S2.3.5. The ^{1}H NMR spectrum of complex **6** in D_2O.

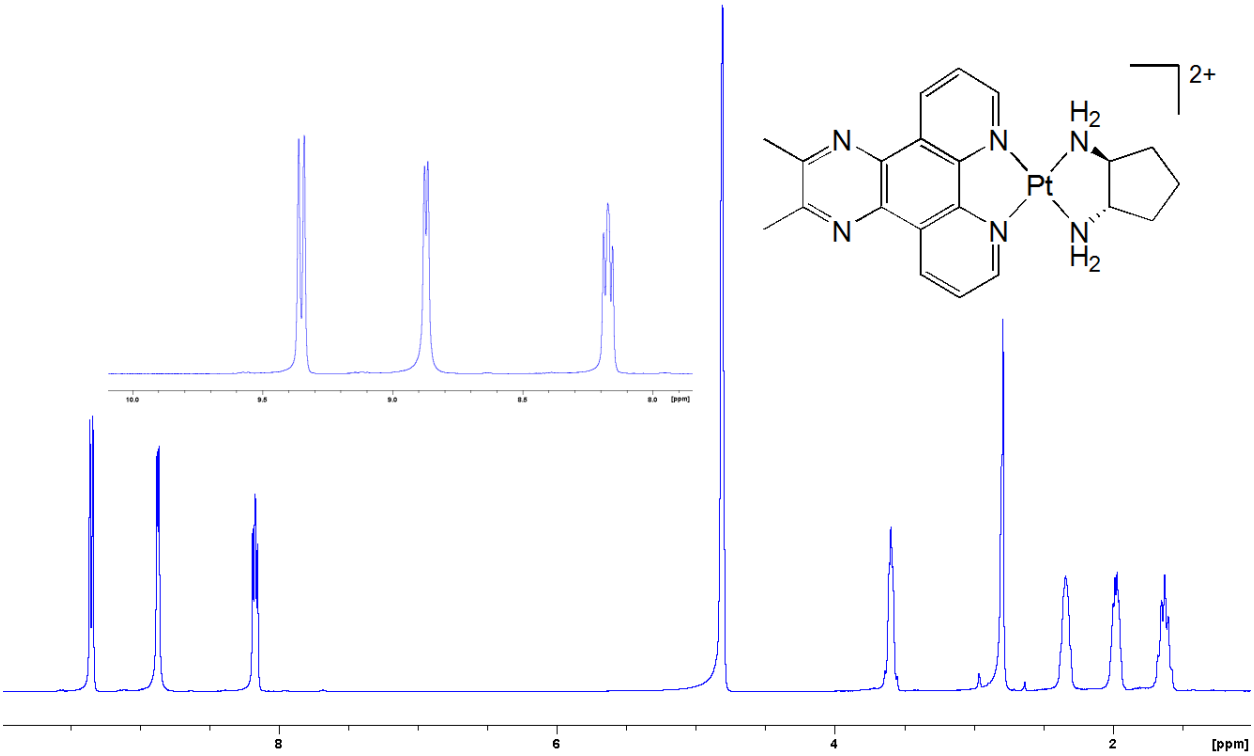

Figure S2.3.6. The ^{1}H NMR spectrum of complex **7** in D_2O.

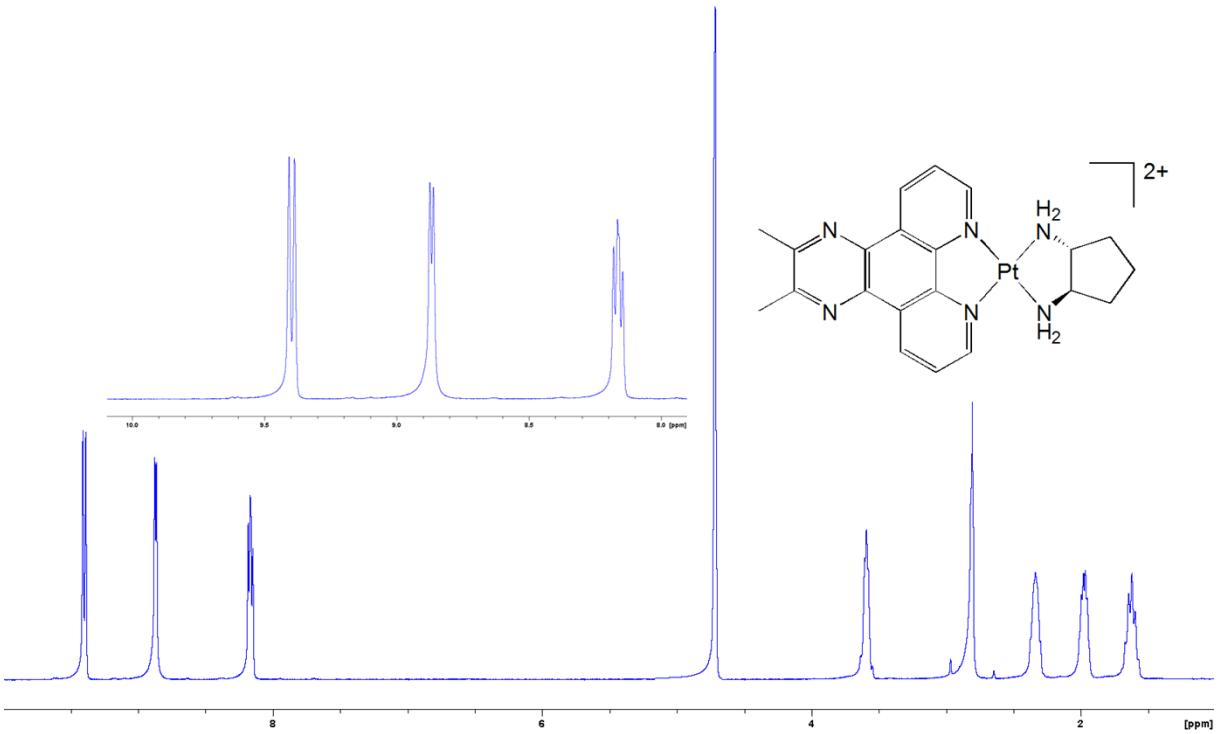

Figure S2.3.7. The ^{1}H NMR spectrum of complex **8** in D_2O.

S2.4. ^{1}H-^{195}Pt HMQC spectra

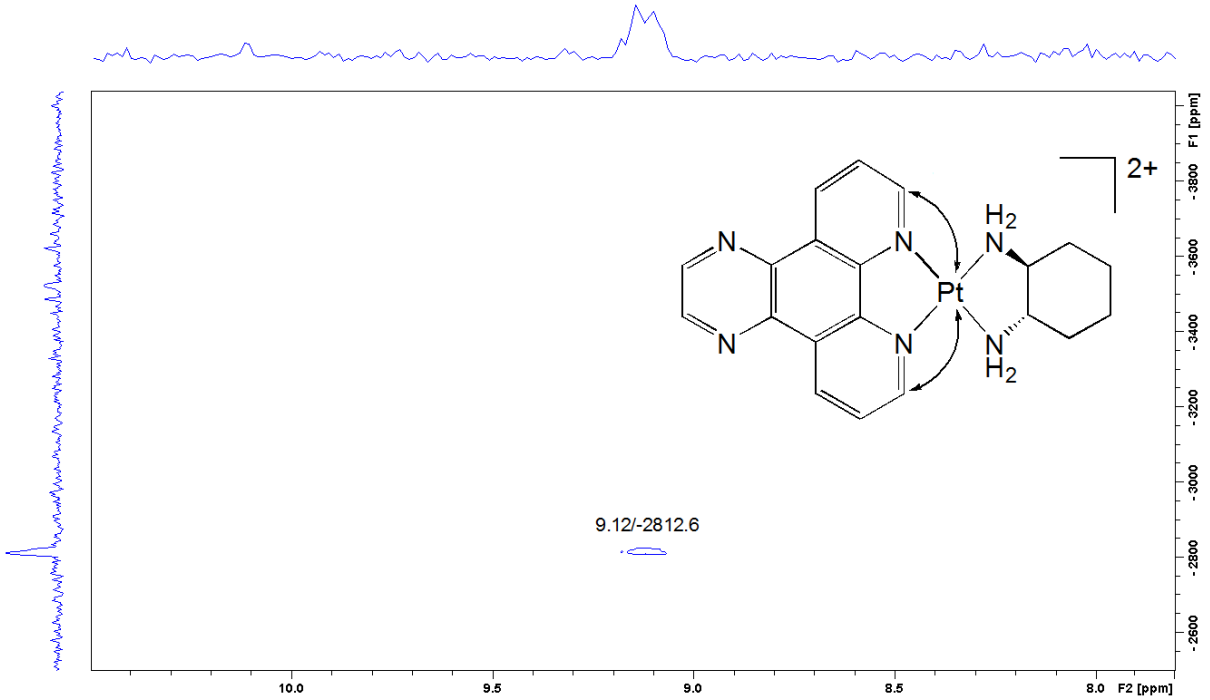

Figure S2.4.1. The ^{1}H-^{195}Pt HMQC spectrum of complex **1** in D_2O.

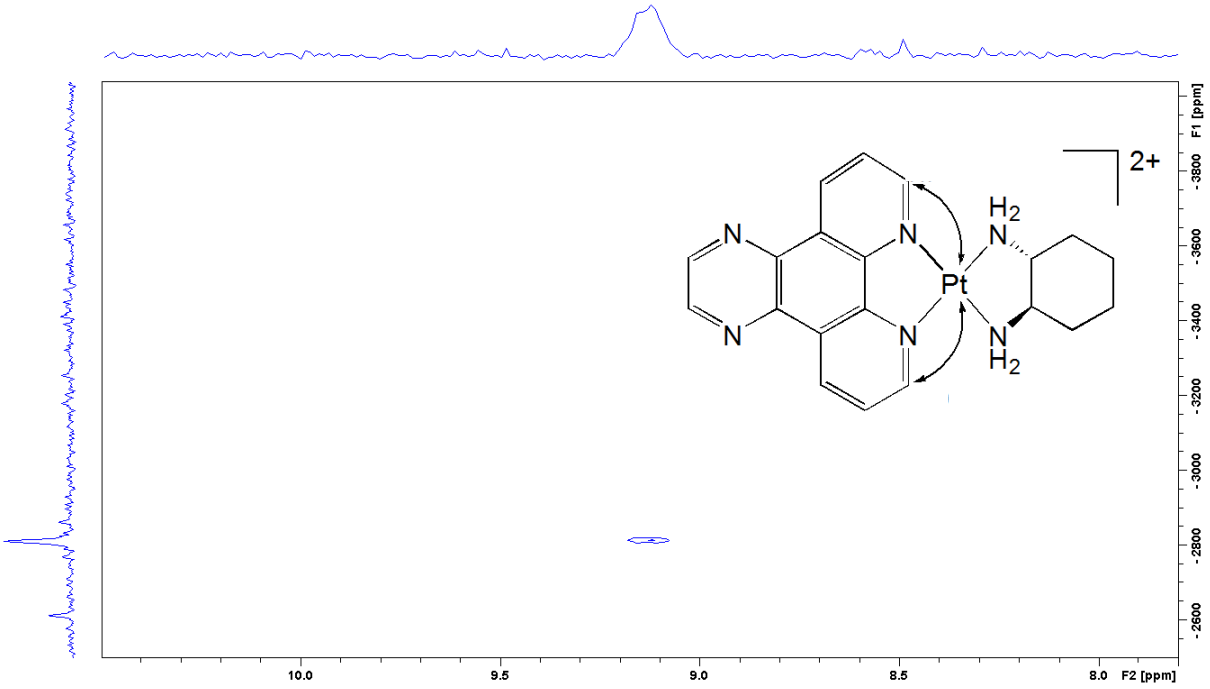

Figure S2.4.2. The ^{1}H-^{195}Pt HMQC spectrum of complex **2** in D_2O.

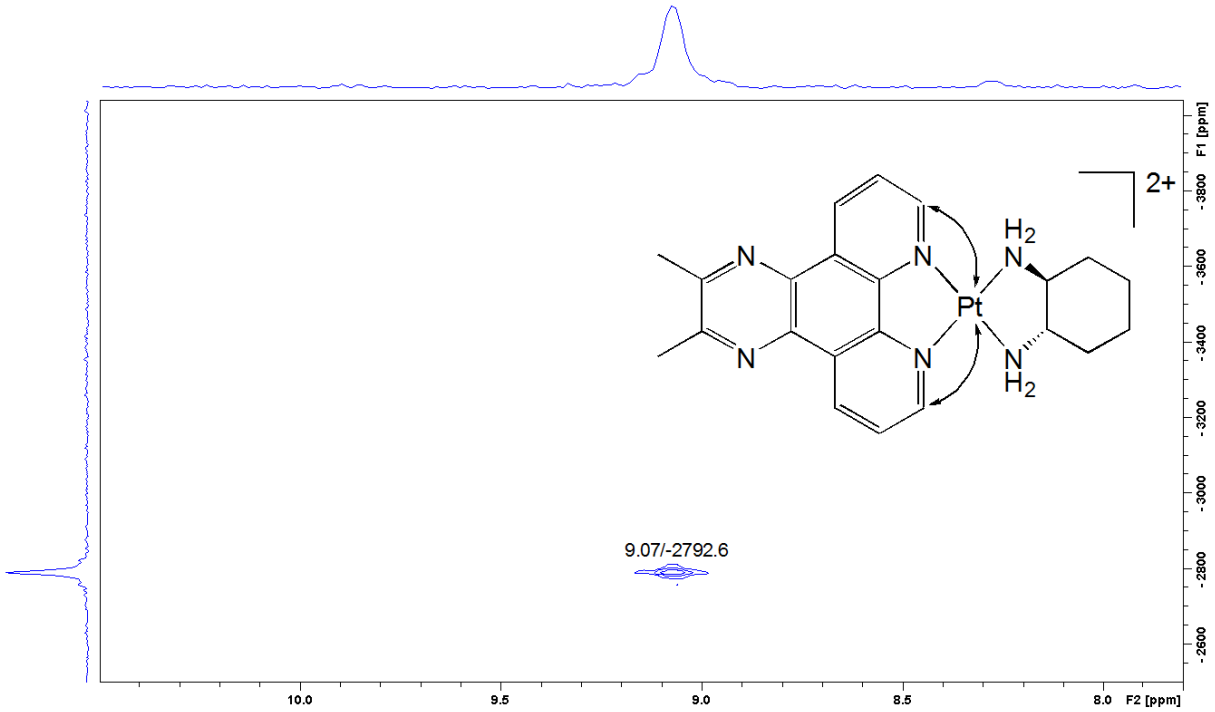

Figure S2.4.3. The ^{1}H-^{195}Pt HMQC spectrum of complex **3** in D_2O.

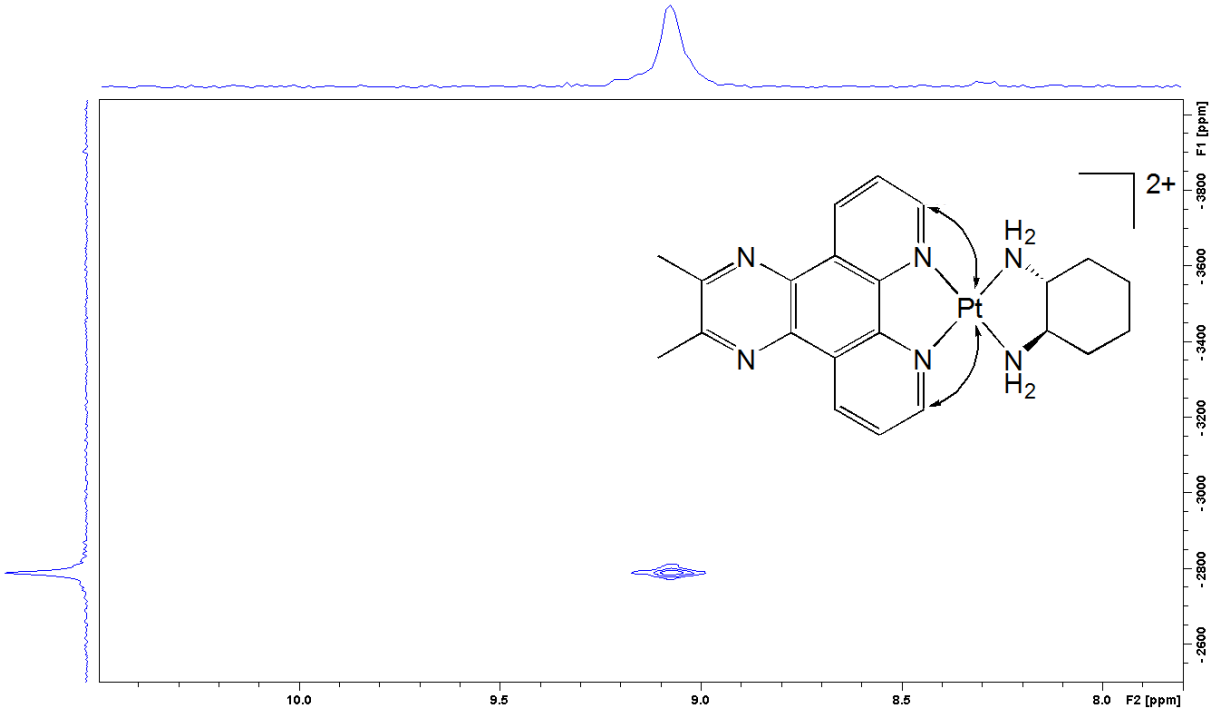

Figure S2.4.4. The ^{1}H-^{195}Pt HMQC spectrum of complex **4** in D_2O.

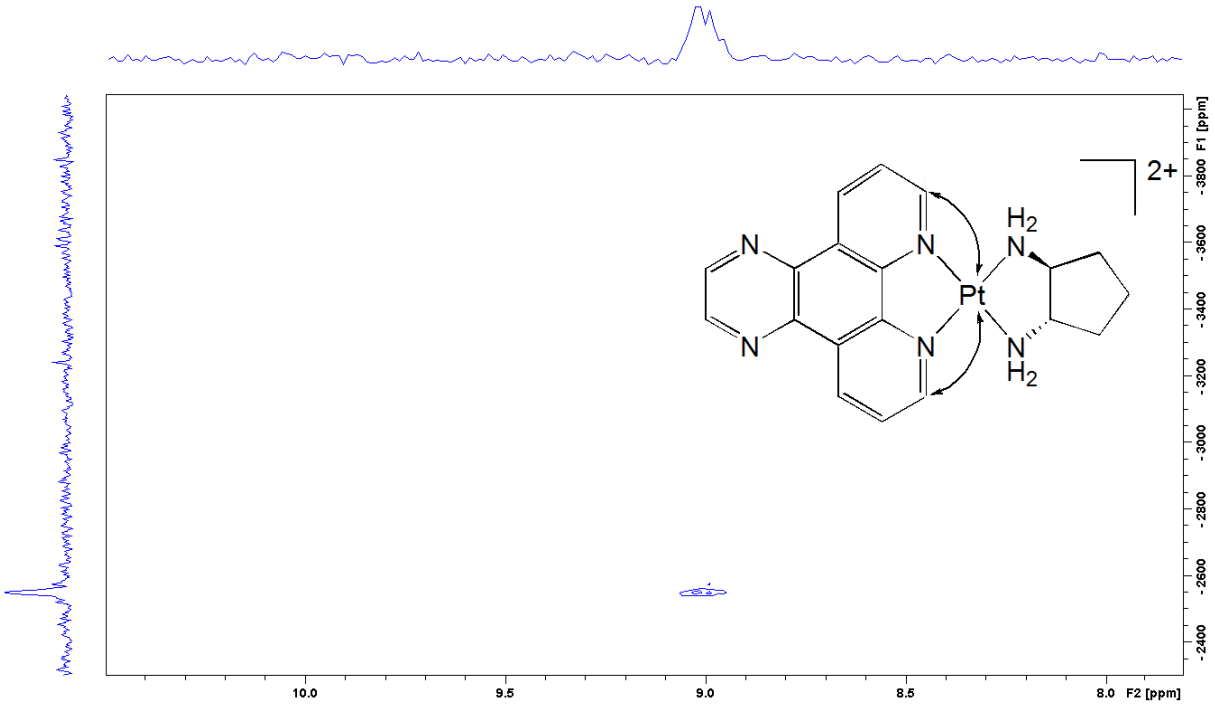

Figure S2.4.5. The ^{1}H-^{195}Pt HMQC spectrum of complex **5** in D_2O. The ^{195}Pt chemical shift is lower than that of complex **1**, as discussed in the main text.

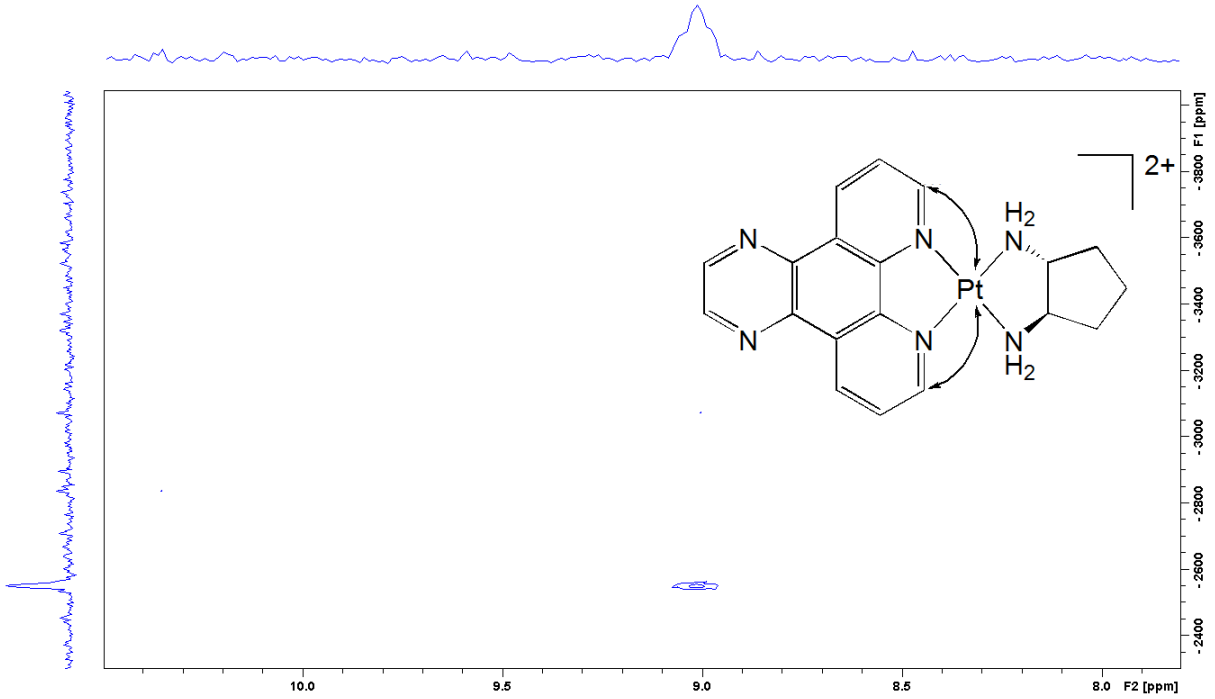

Figure S2.4.6. The ^{1}H-^{195}Pt HMQC spectrum of complex **6** in D_2O.

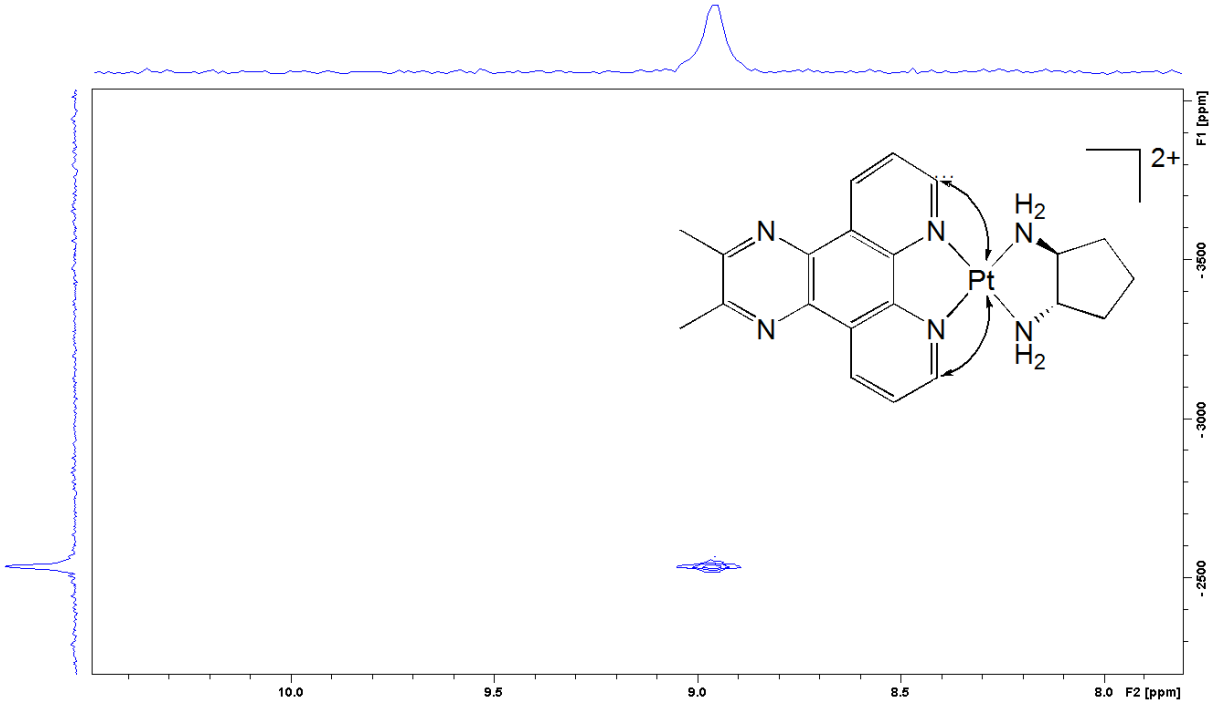

Figure S2.4.7. The ^{1}H-^{195}Pt HMQC spectrum of complex **7** in D_2O.

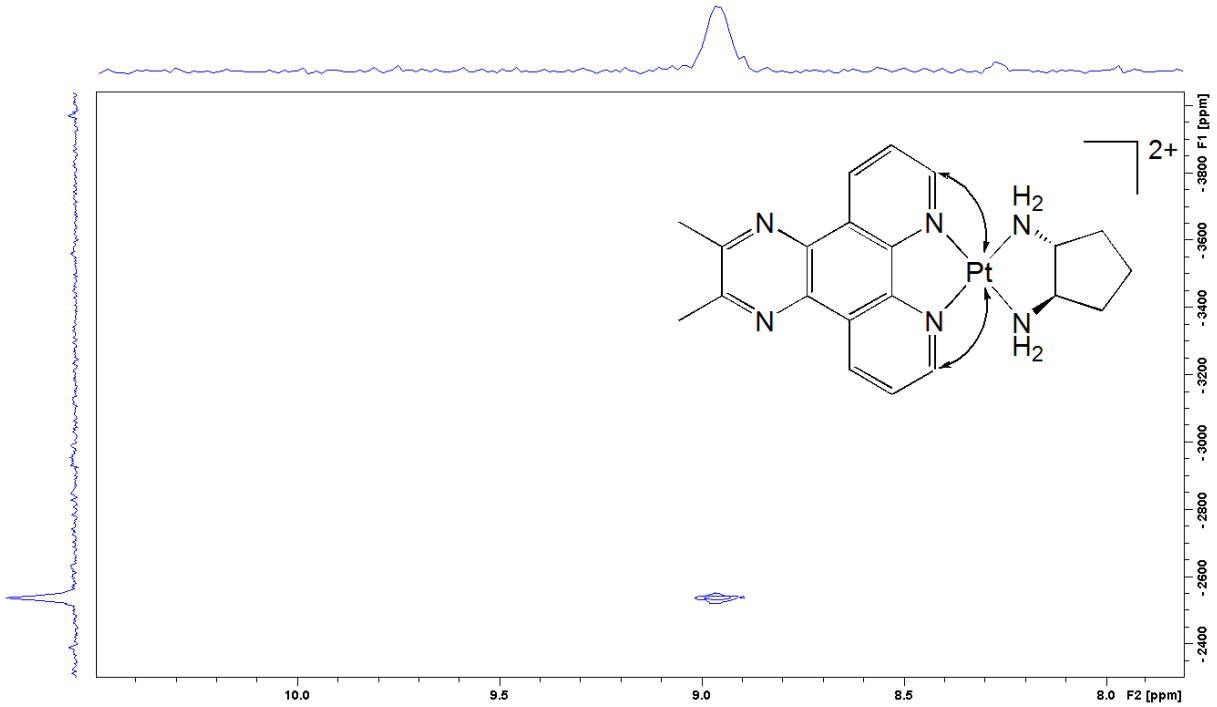

Figure S2.4.8. The ^{1}H-^{195}Pt HMQC spectrum of complex **8** in D_2O.

S2.5. Electrospray Ionisation Mass Spectra

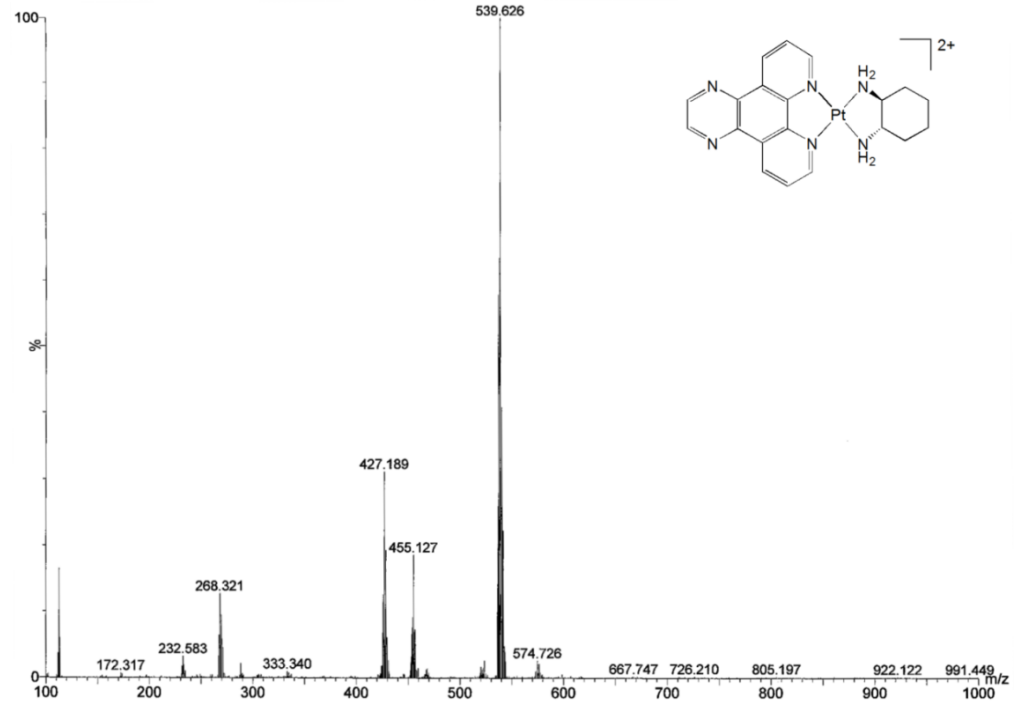

Figure S2.5.1. The mass spectrum of complex **1**.

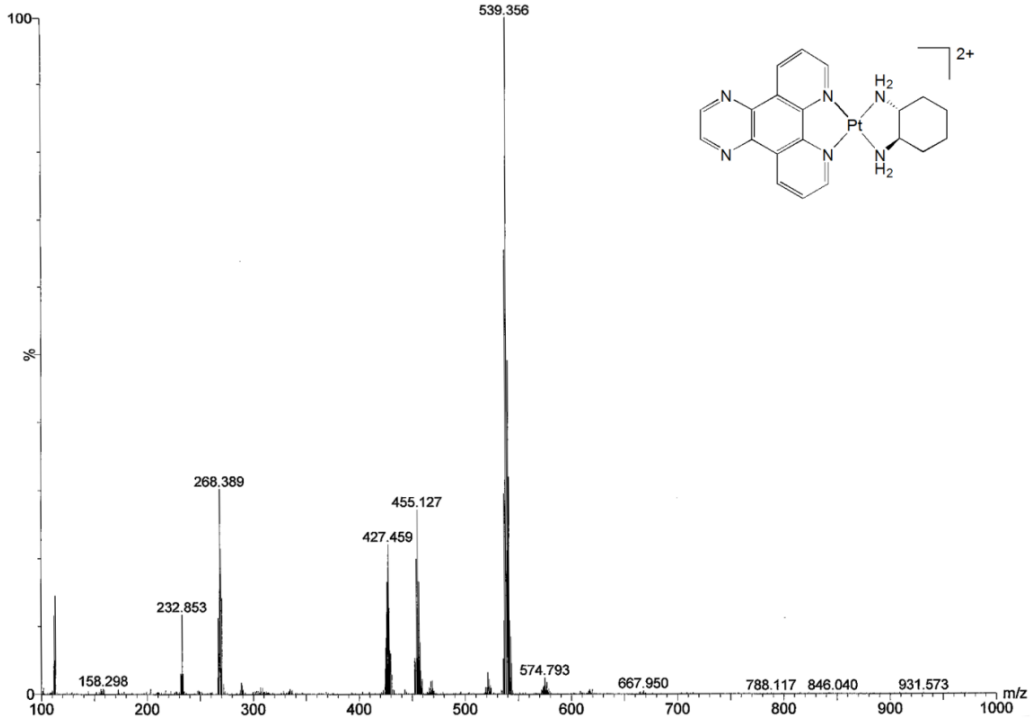

Figure S2.5.2. The mass spectrum of complex **2**.

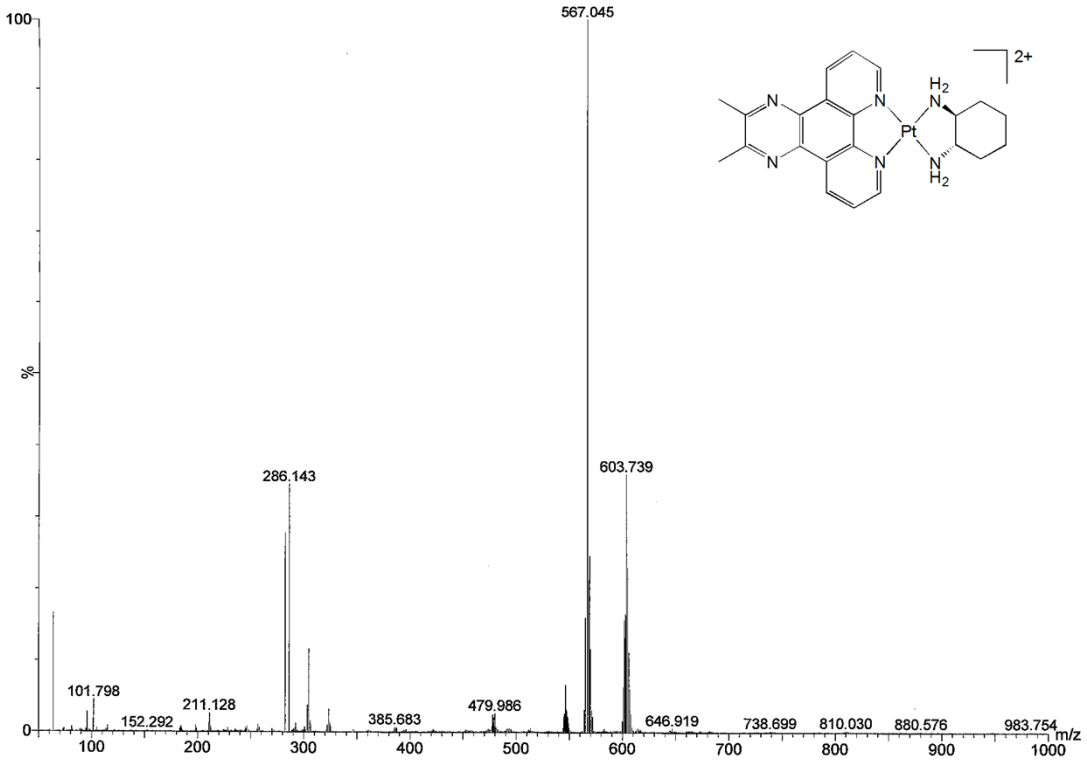

Figure S2.5.3. The mass spectrum of complex **3**

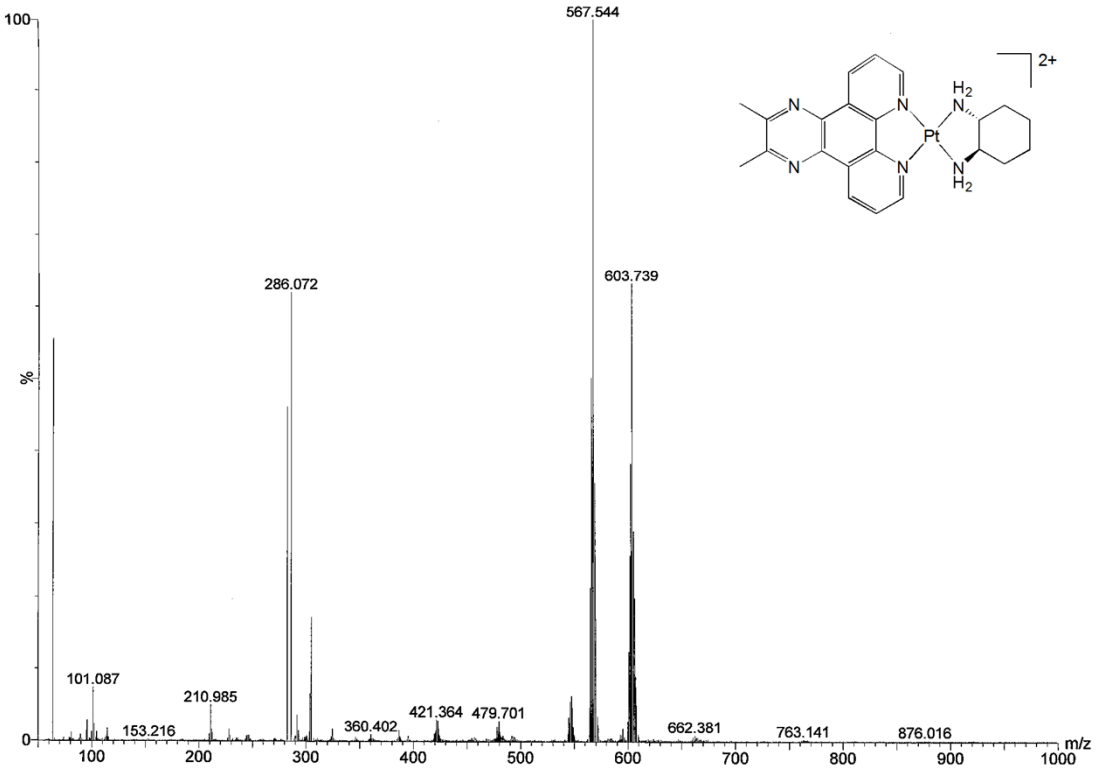

Figure S2.5.4. The mass spectrum of complex **4**.

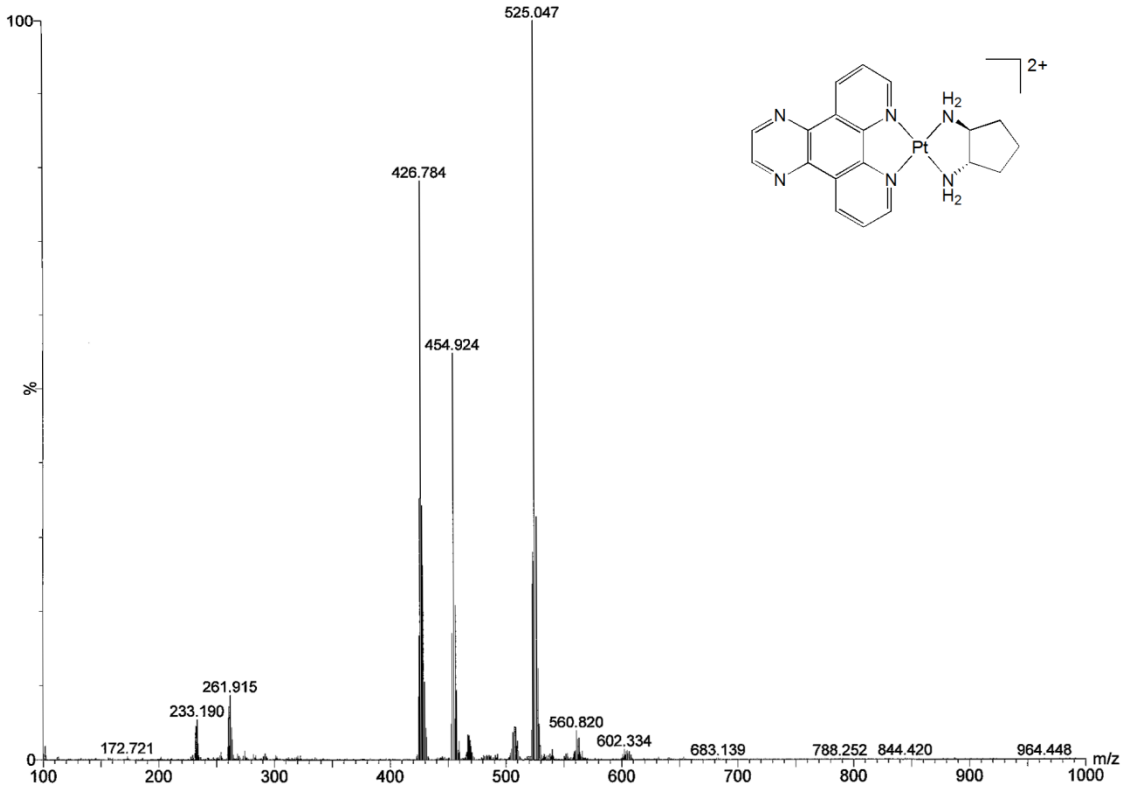

Figure S2.5.5. The mass spectrum of complex **5**.

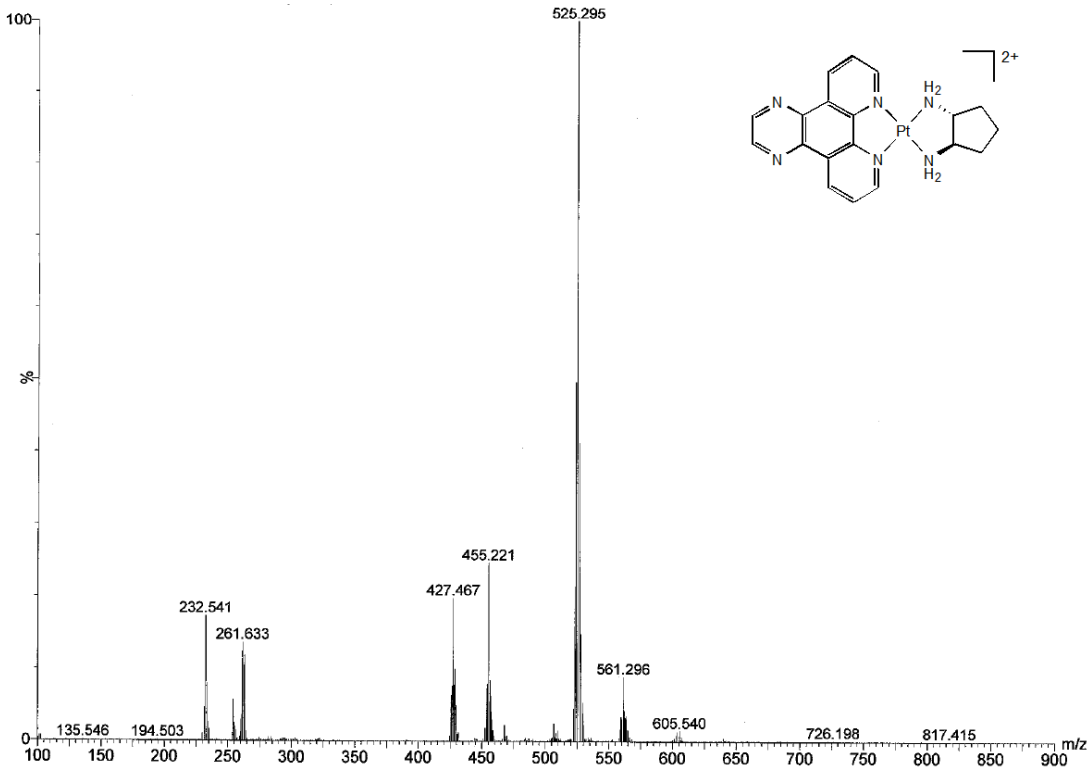

Figure S2.5.6. The mass spectrum of complex **6**.

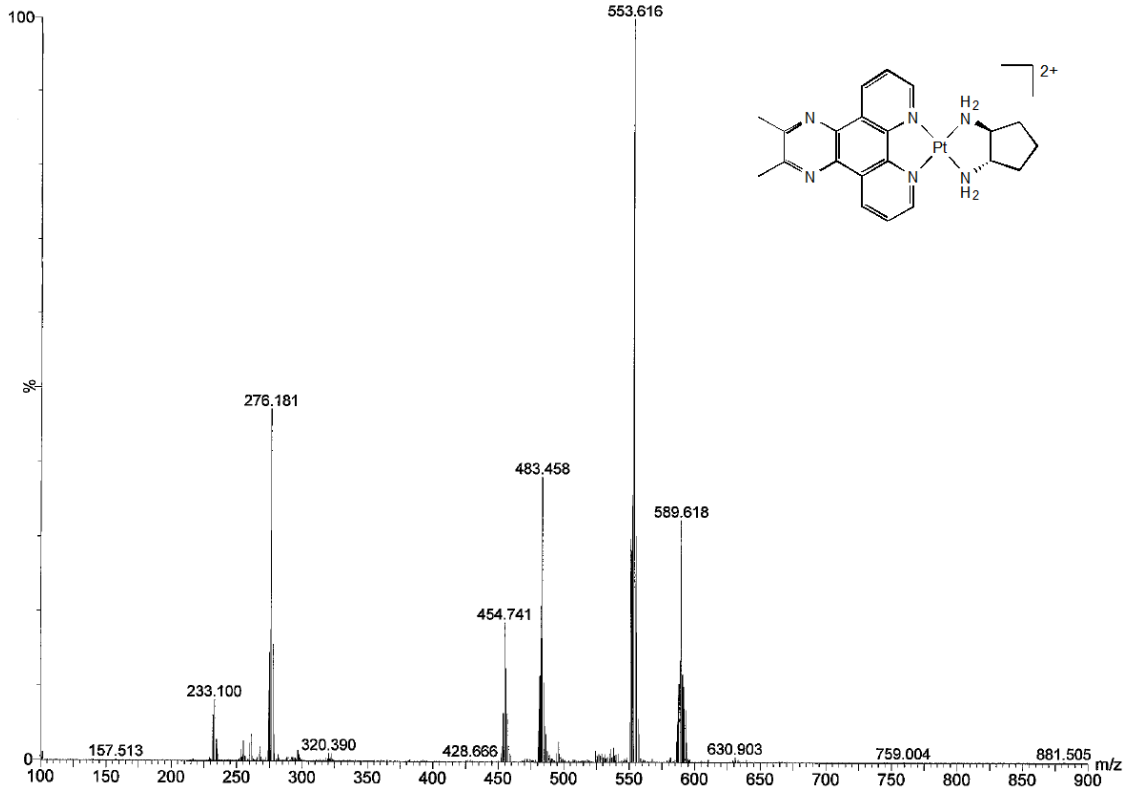

Figure S2.5.7. The mass spectrum of complex **7**.

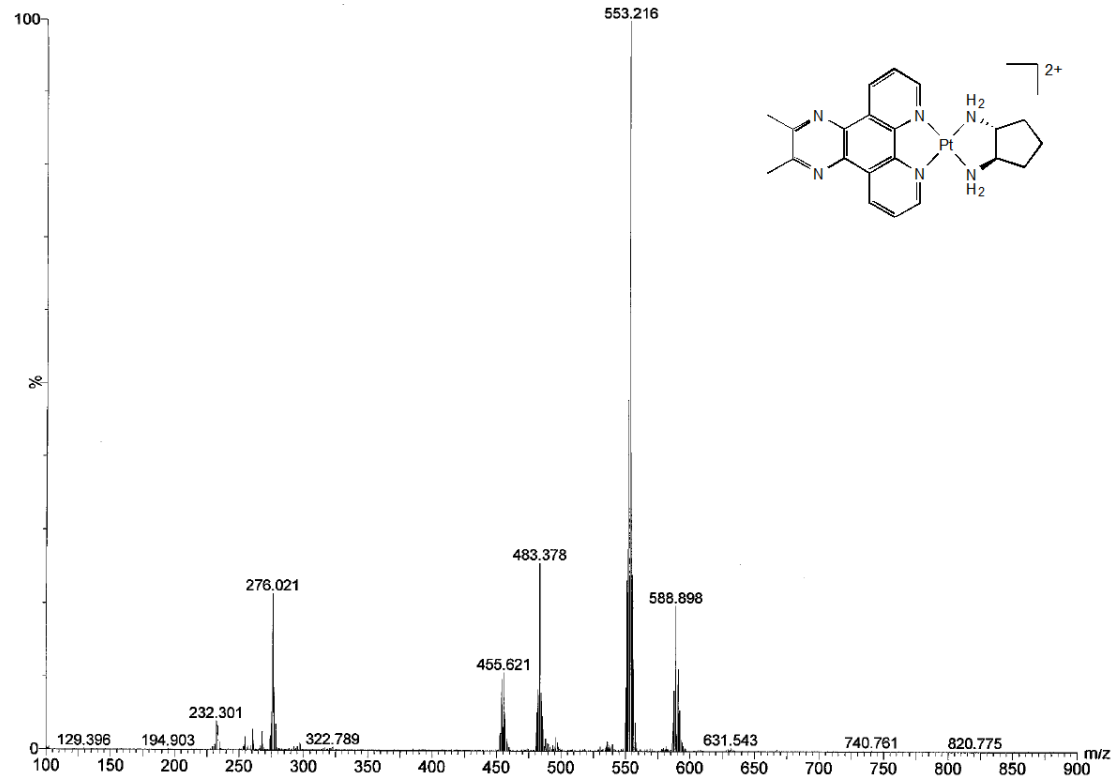

Figure S2.5.8. The mass spectrum of complex **8**.

S2.6. HPLC Traces

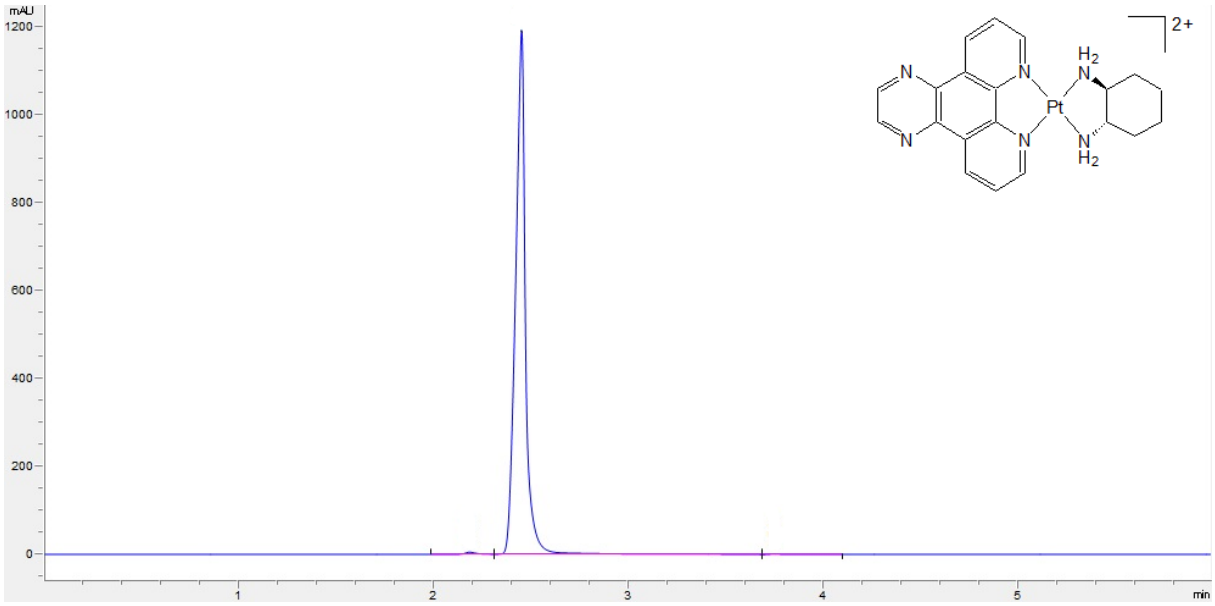

Figure S2.6.1. The HPLC trace of complex **1**.

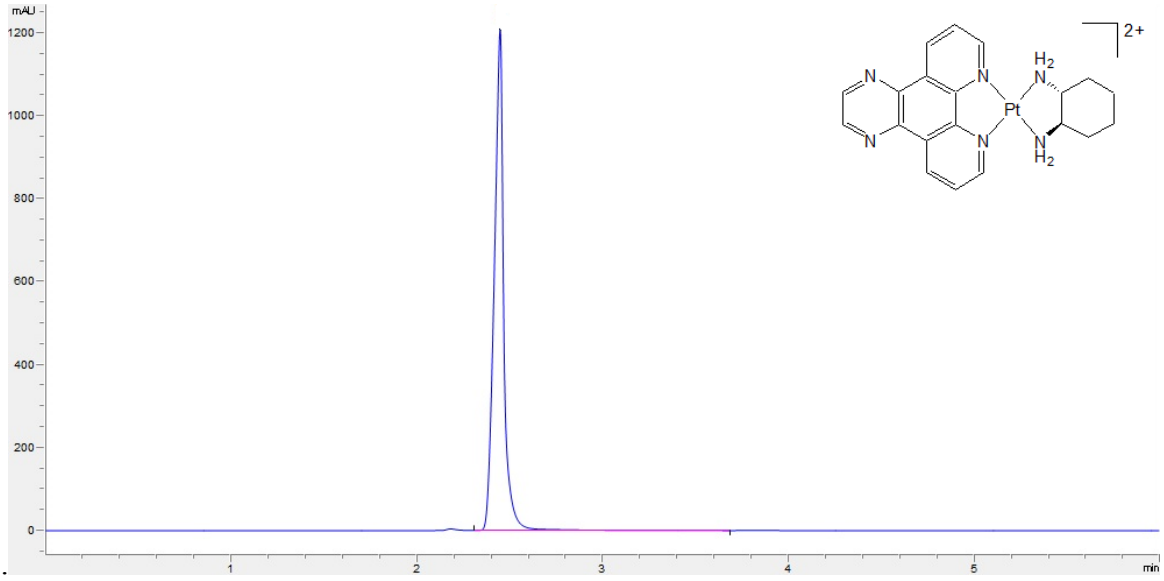

Figure S2.6.2. The HPLC trace of complex **2**.

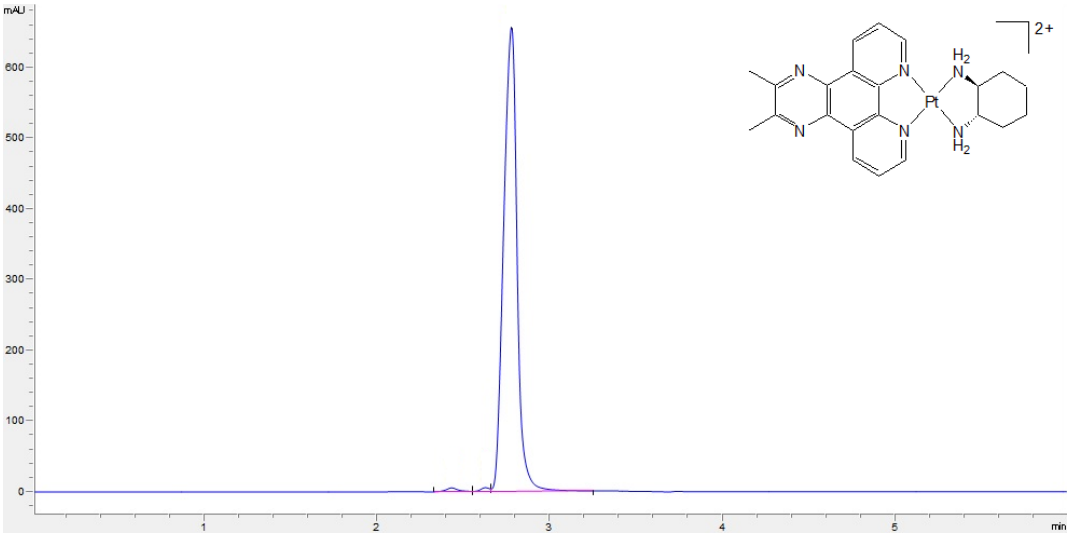

Figure S2.6.3. The HPLC trace of complex **3**.

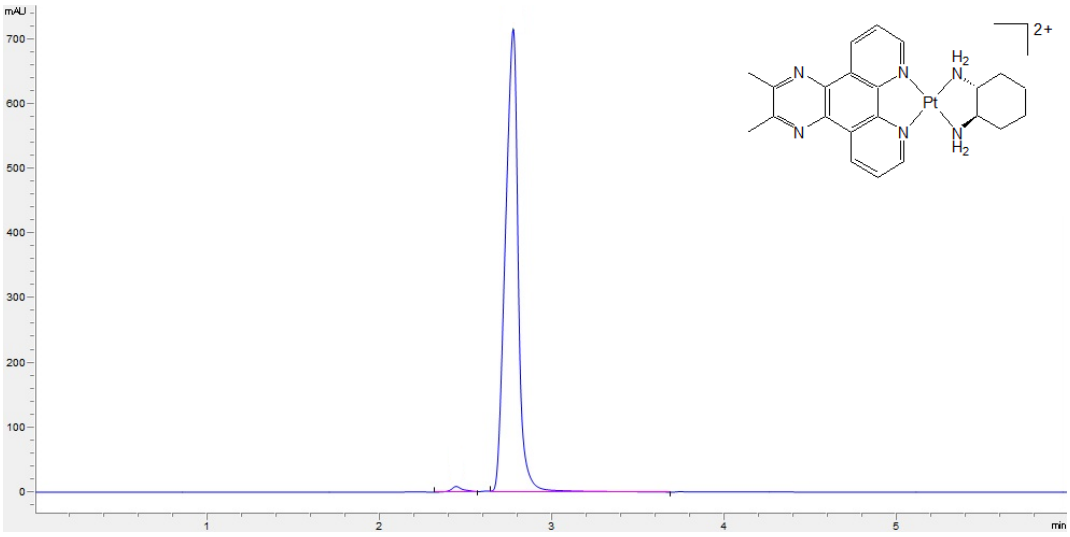

Figure S2.6.4. The HPLC trace of complex **4**.

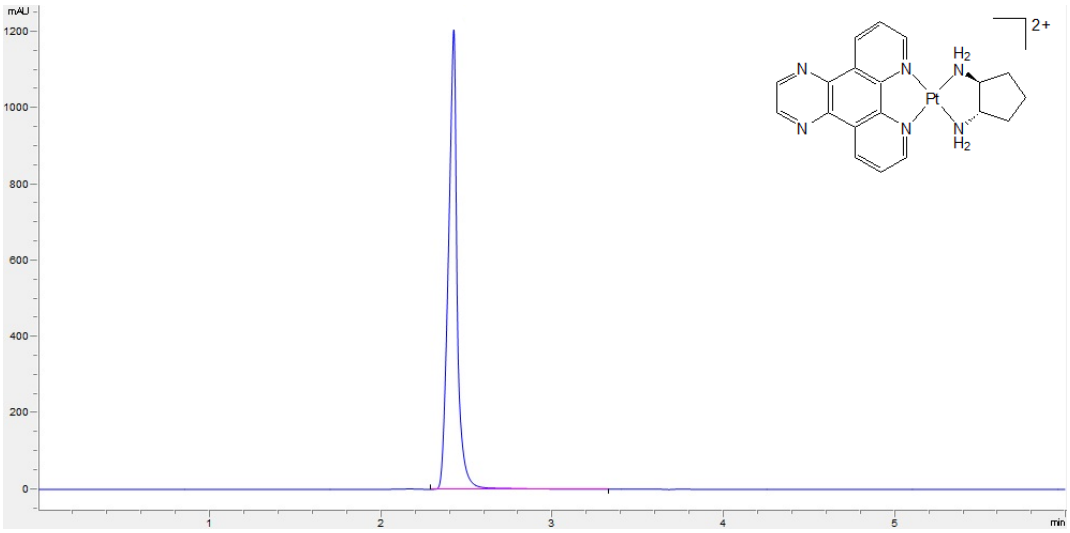

Figure S2.6.5. The HPLC trace of complex **5**.

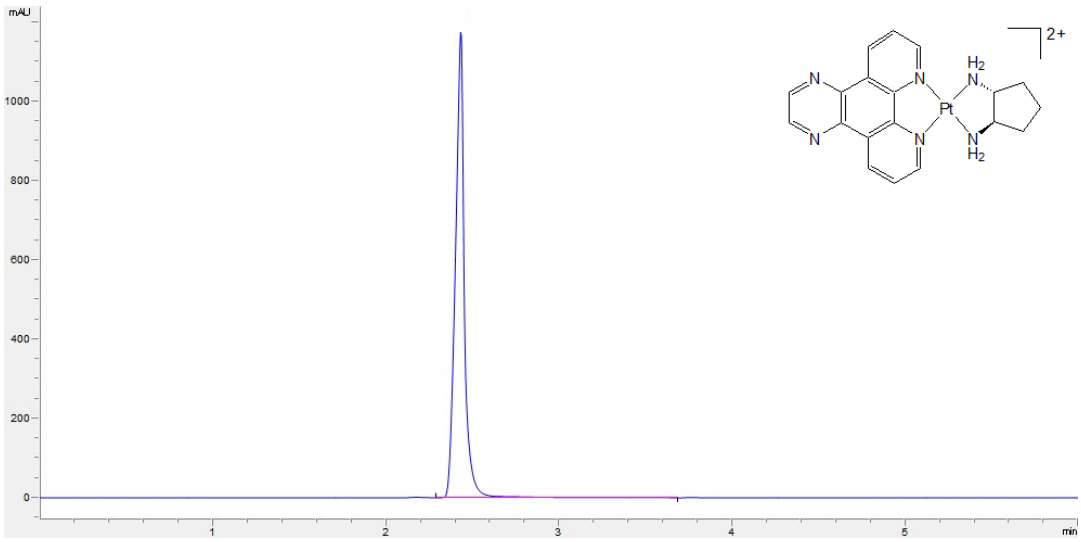

Figure S2.6.6. The HPLC trace of complex **6**.

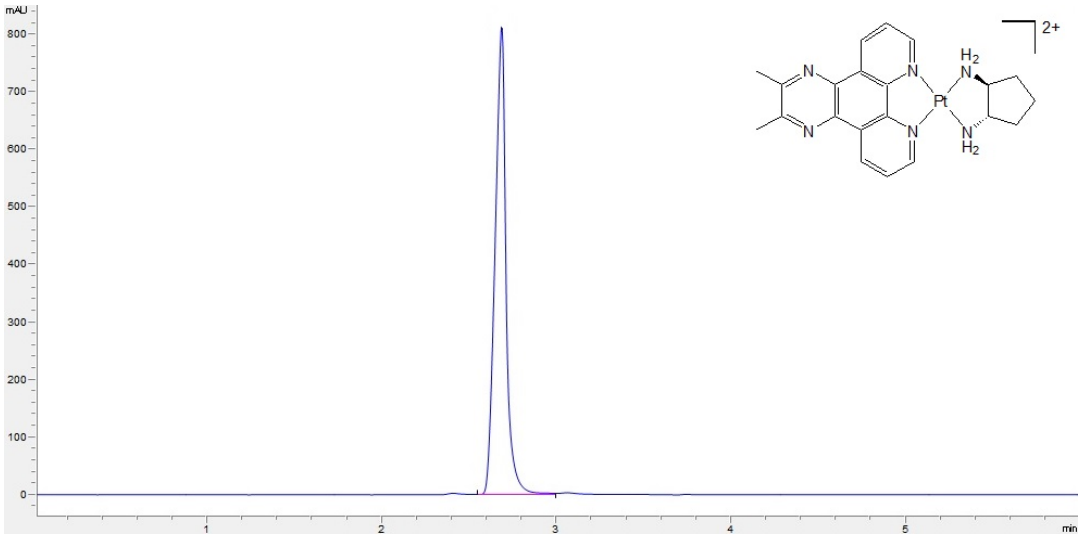

Figure S2.6.7. The HPLC trace of complex **7**.

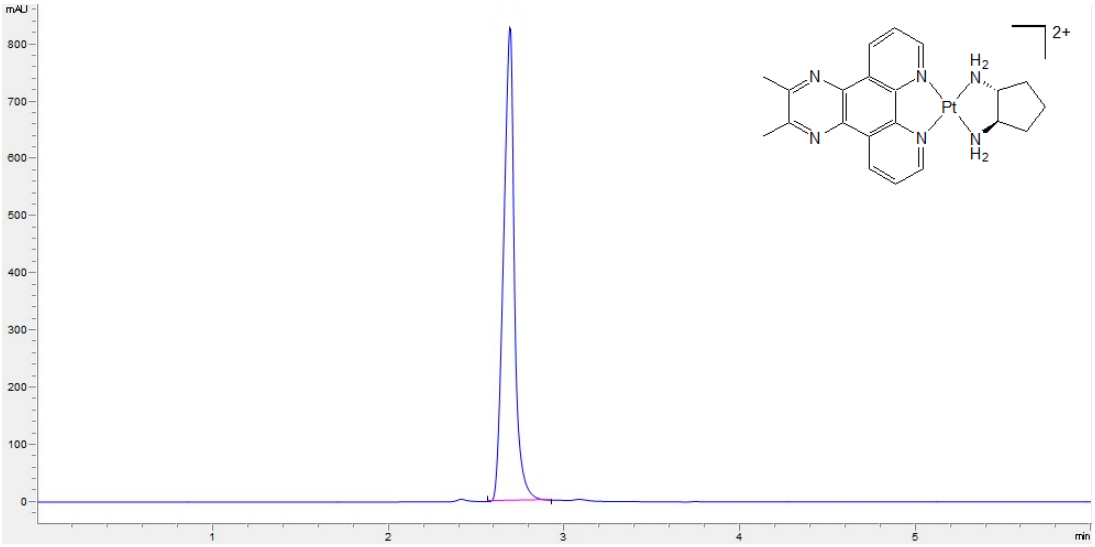

Figure S2.6.8. The HPLC trace of complex **8**.

Section S3 – Fluorescence Data

S3.1. Solution composition

Table S3.1. Summary of the metal complex titration solutions used. For each complex, these solutions were loaded into a 96-well plate for testing. [PC solution 1] = 16.3 μM, [PC solution 2] = 122.5 μM. Two different PC solutions were utilised to minimise pipette volume error.

Sample No.	EtBr / μL	[EtBr] / μM	DNA / μL	[DNA] / μM	PC solution 1 / μL	PC solution 2 / μL	[PC] / μM	Buffer	Total Volume / μL	[DNA]:[PC]
1	20	29.40	0	0	0	0	0	290	300	-
2	20	29.40	100	73.45	0	0	0	90	300	-
3	20	29.40	100	73.45	27	0	1.47	63	300	50
4	20	29.40	100	73.45	38	0	2.07	52	300	35
5	20	29.40	100	73.45	67	0	3.65	23	300	20
6	20	29.40	100	73.45	90	0	4.90	0	300	15
7	20	29.40	100	73.45	0	18	7.35	81	300	10
8	20	29.40	100	73.45	0	24	9.80	78	300	7
9	20	29.40	100	73.45	0	36	14.70	72	300	5
10	20	29.40	100	73.45	0	60	24.50	60	300	3
11	20	29.40	100	73.45	0	180	73.45	0	300	1

S3.2. Data Summary by Compound

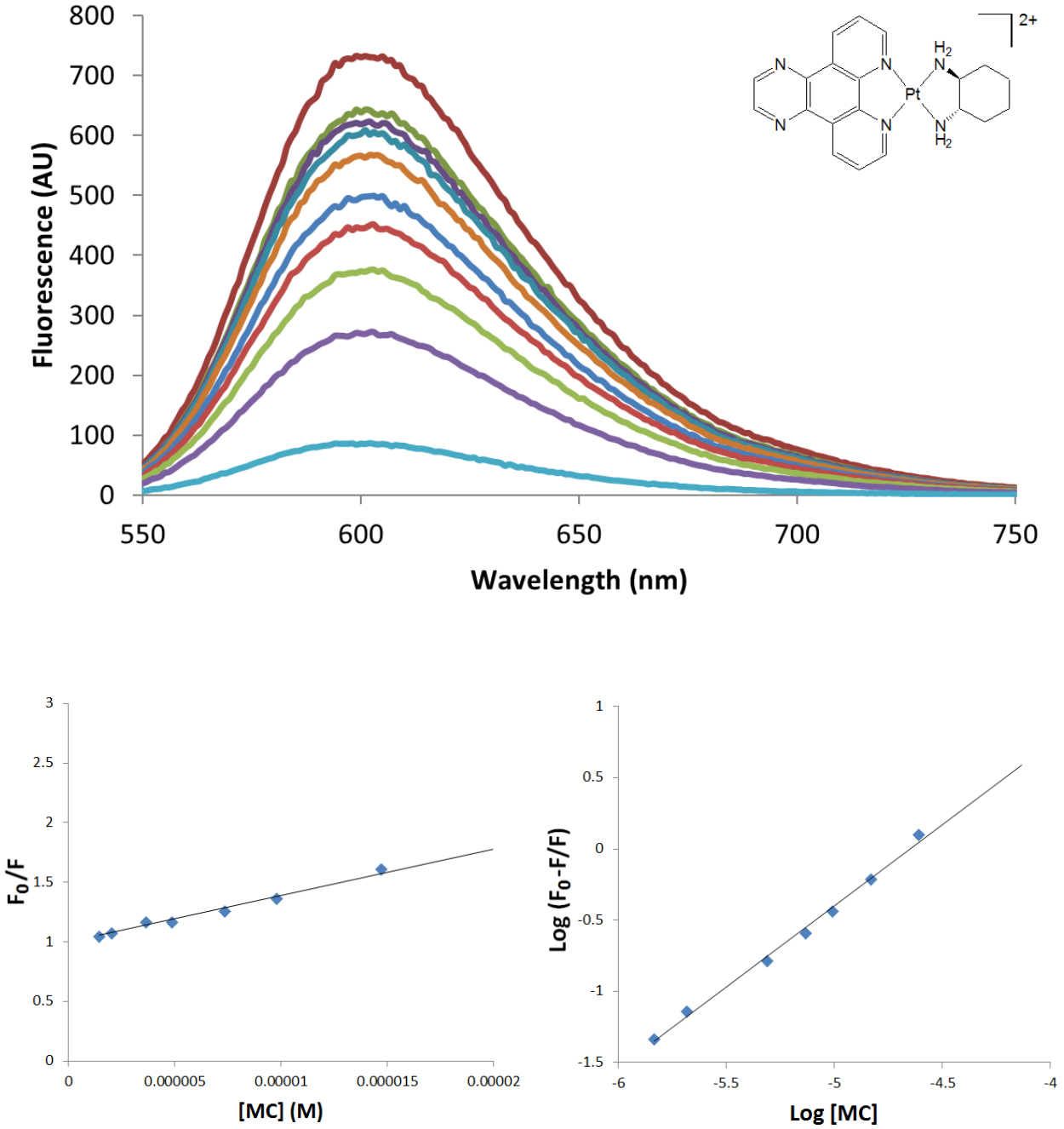

Figure S3.2.1. Fluorescence binding data for complex **1**, obtained from the first duplicate used: the emission spectra (top), Stern-Volmer plot (bottom left), and double-logarithm plot (bottom right).

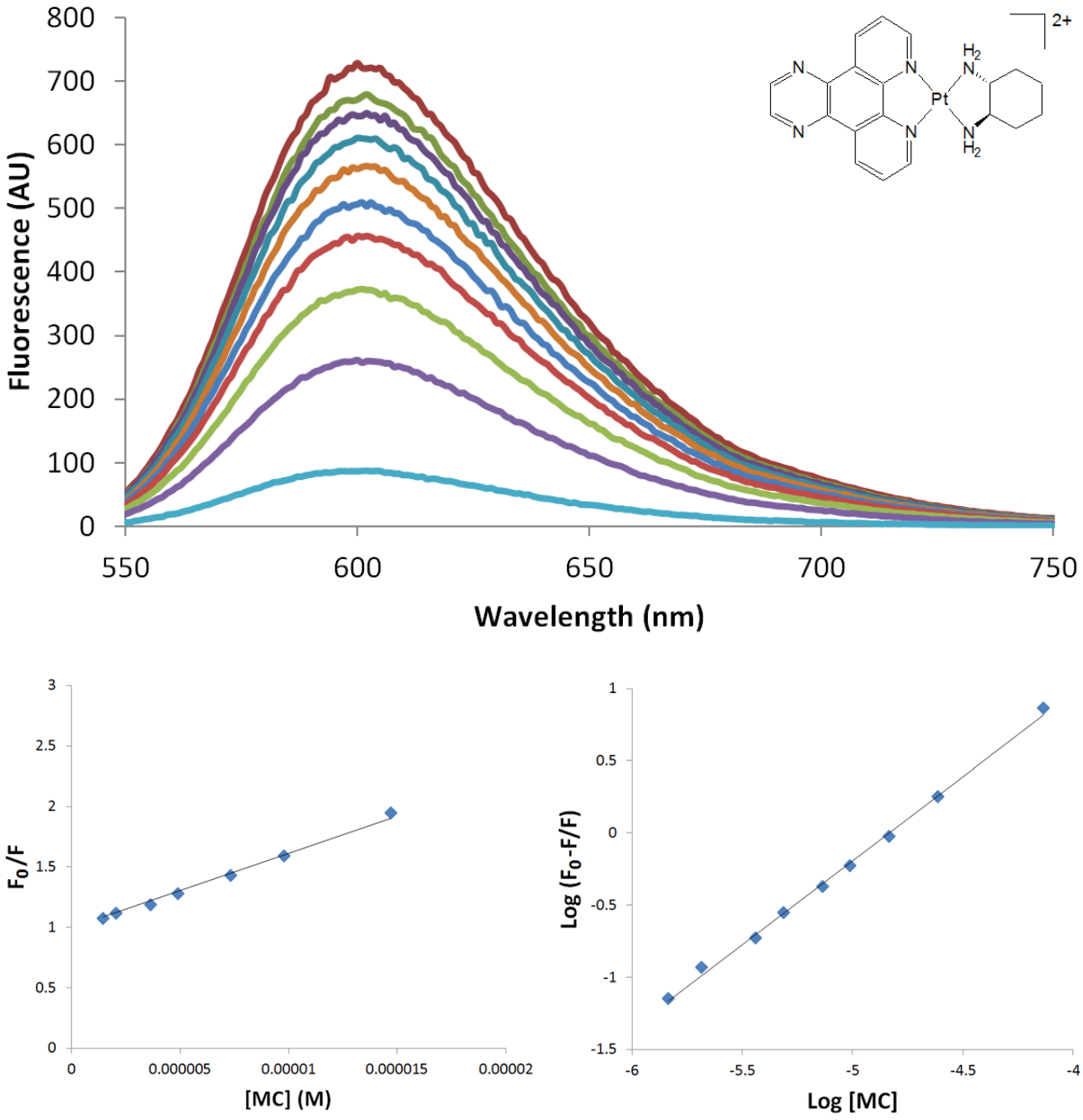

Figure S3.2.2. Fluorescence binding data for complex **2**, obtained from the first duplicate used: the emission spectra (top), Stern-Volmer plot (bottom left), and double-logarithm plot (bottom right).

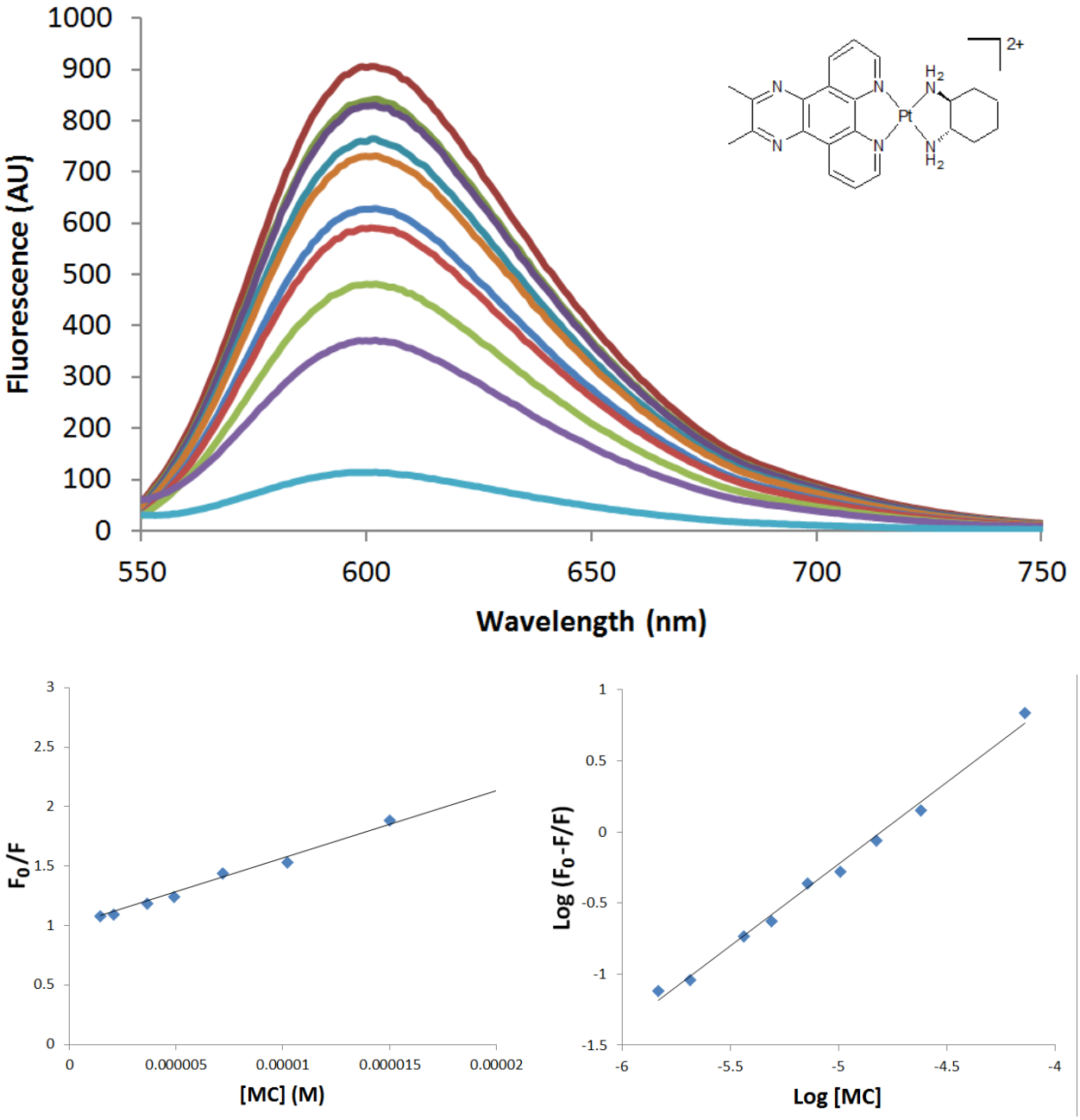

Figure S3.2.3. Fluorescence binding data for complex **3**, obtained from the first duplicate used: the emission spectra (top), Stern-Volmer plot (bottom left), and double-logarithm plot (bottom right).

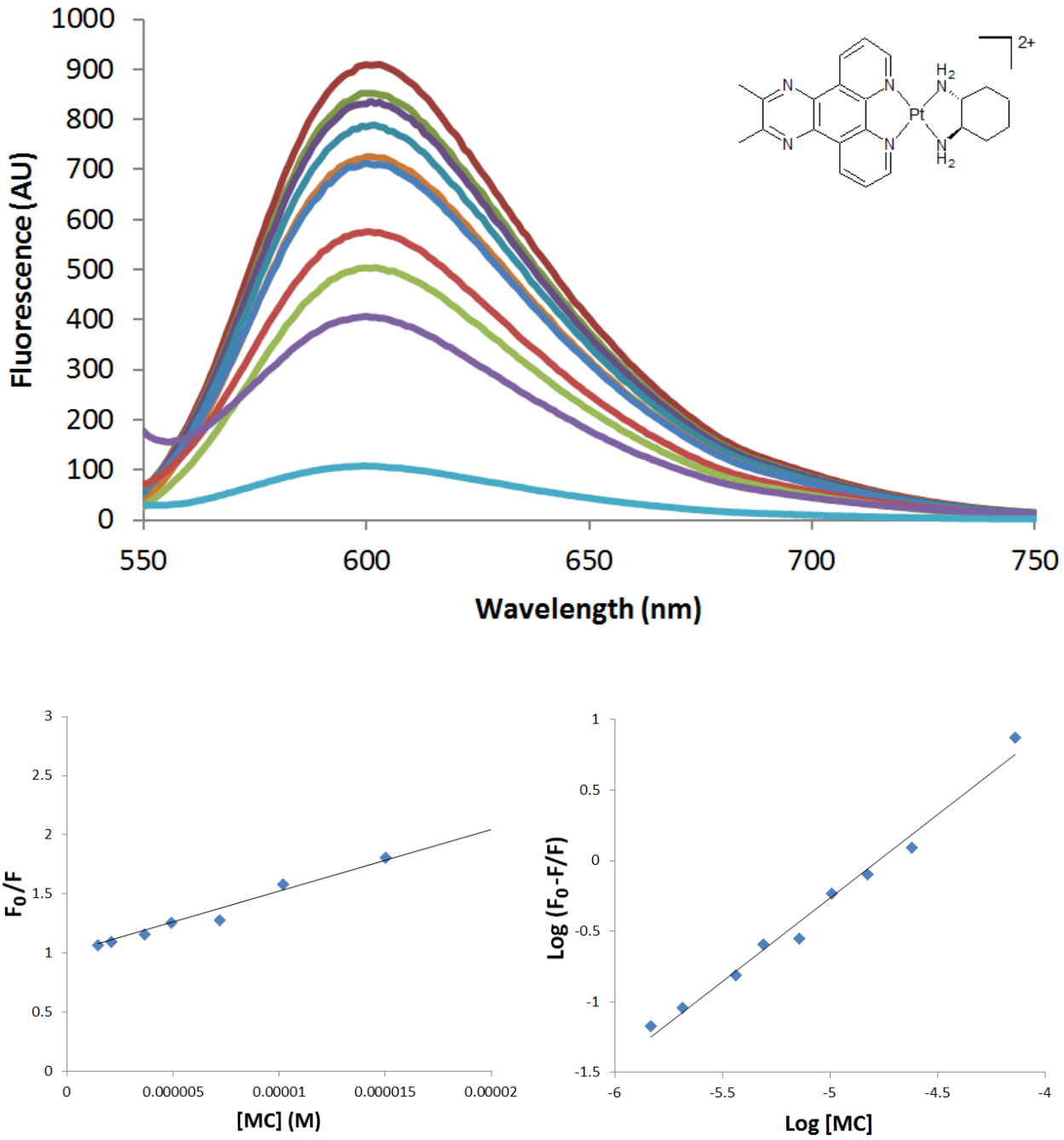

Figure S3.2.4. Fluorescence binding data for complex **4**, obtained from the first duplicate used: the emission spectra (top), Stern-Volmer plot (bottom left), and double-logarithm plot (bottom right).

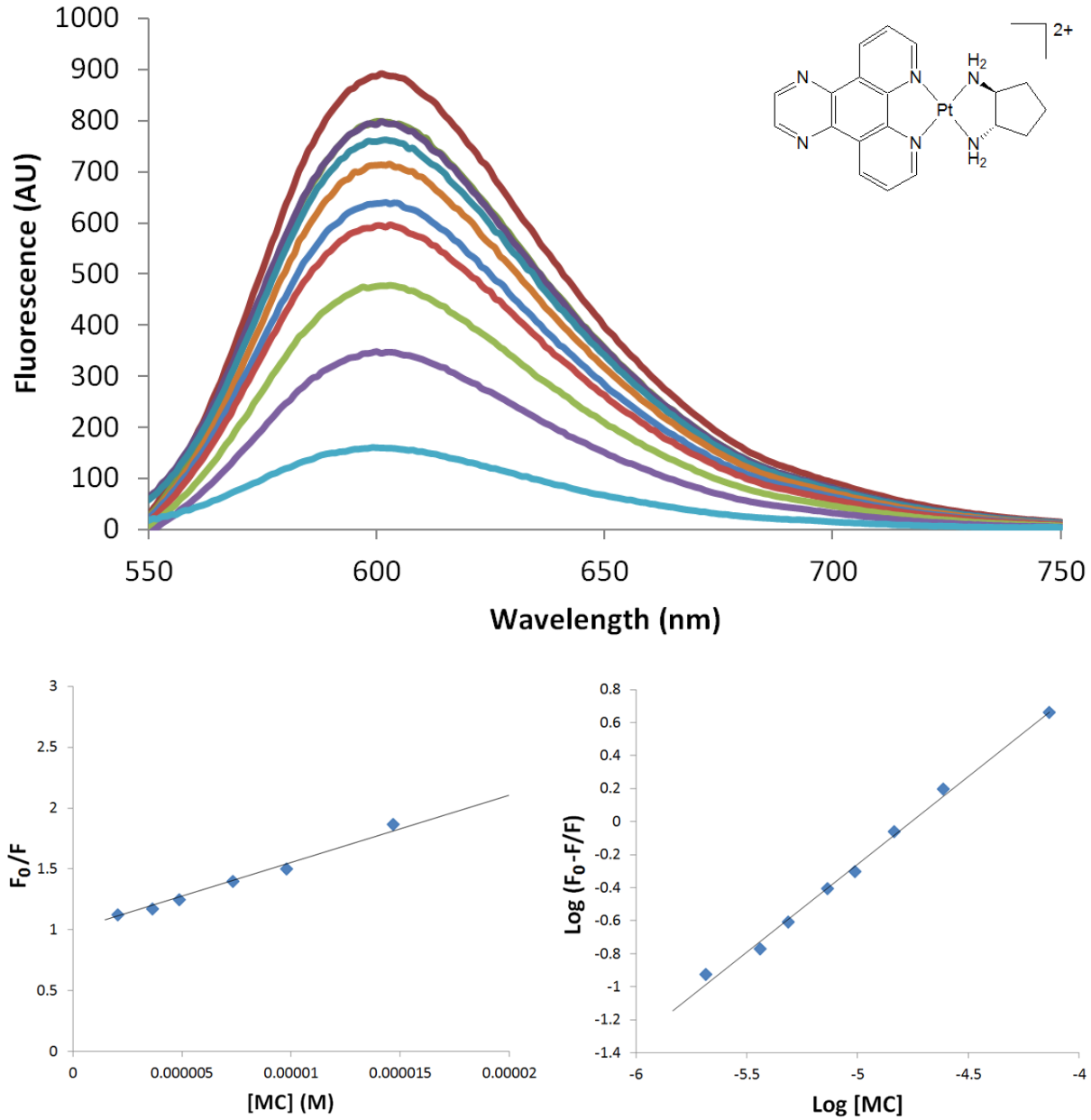

Figure S3.2.5. Fluorescence binding data for complex **5**, obtained from the first duplicate used: the emission spectra (top), Stern-Volmer plot (bottom left), and double-logarithm plot (bottom right).

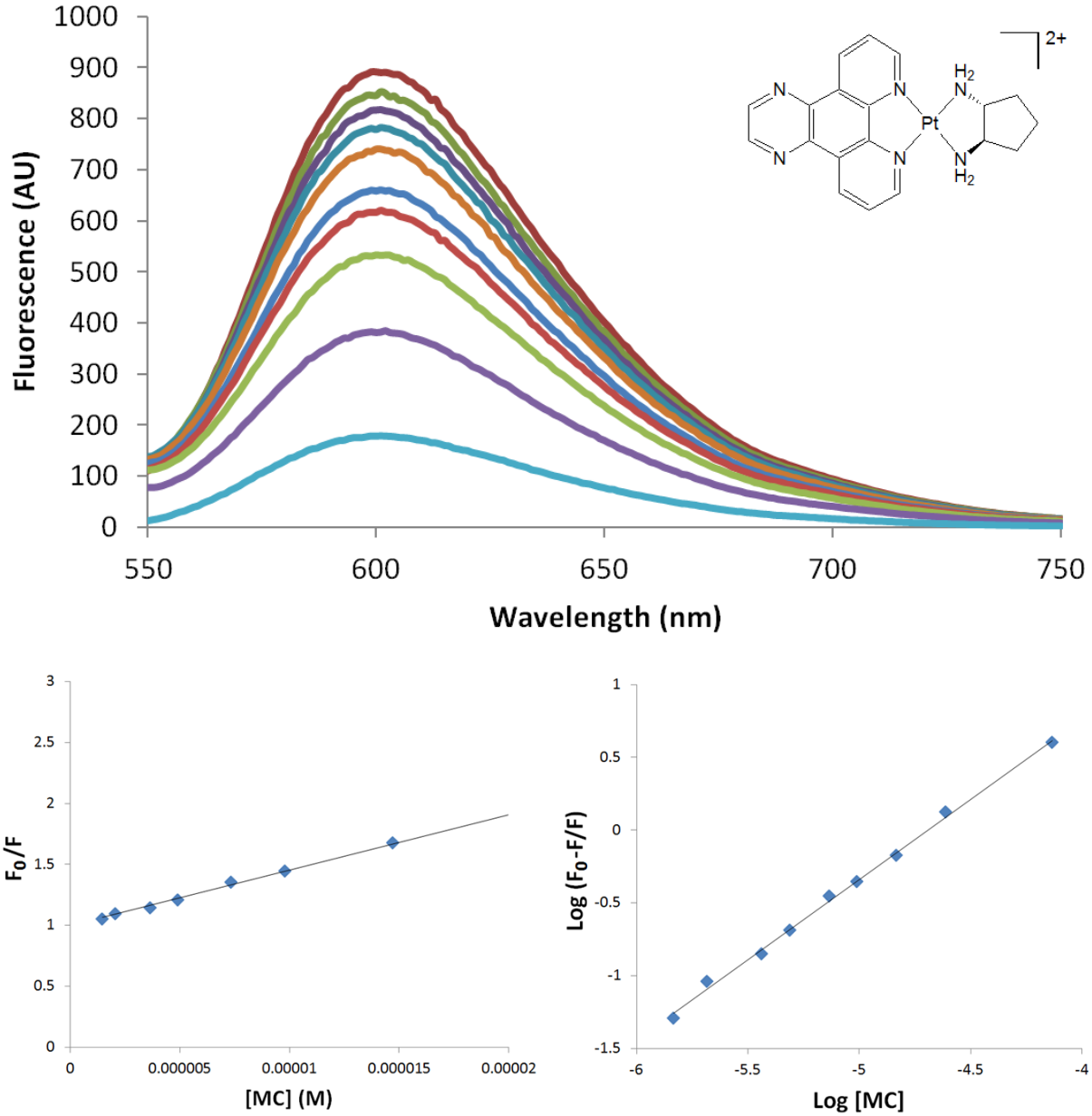

Figure S3.2.6. Fluorescence binding data for complex **6**, obtained from the first duplicate used: the emission spectra (top), Stern-Volmer plot (bottom left), and double-logarithm plot (bottom right).

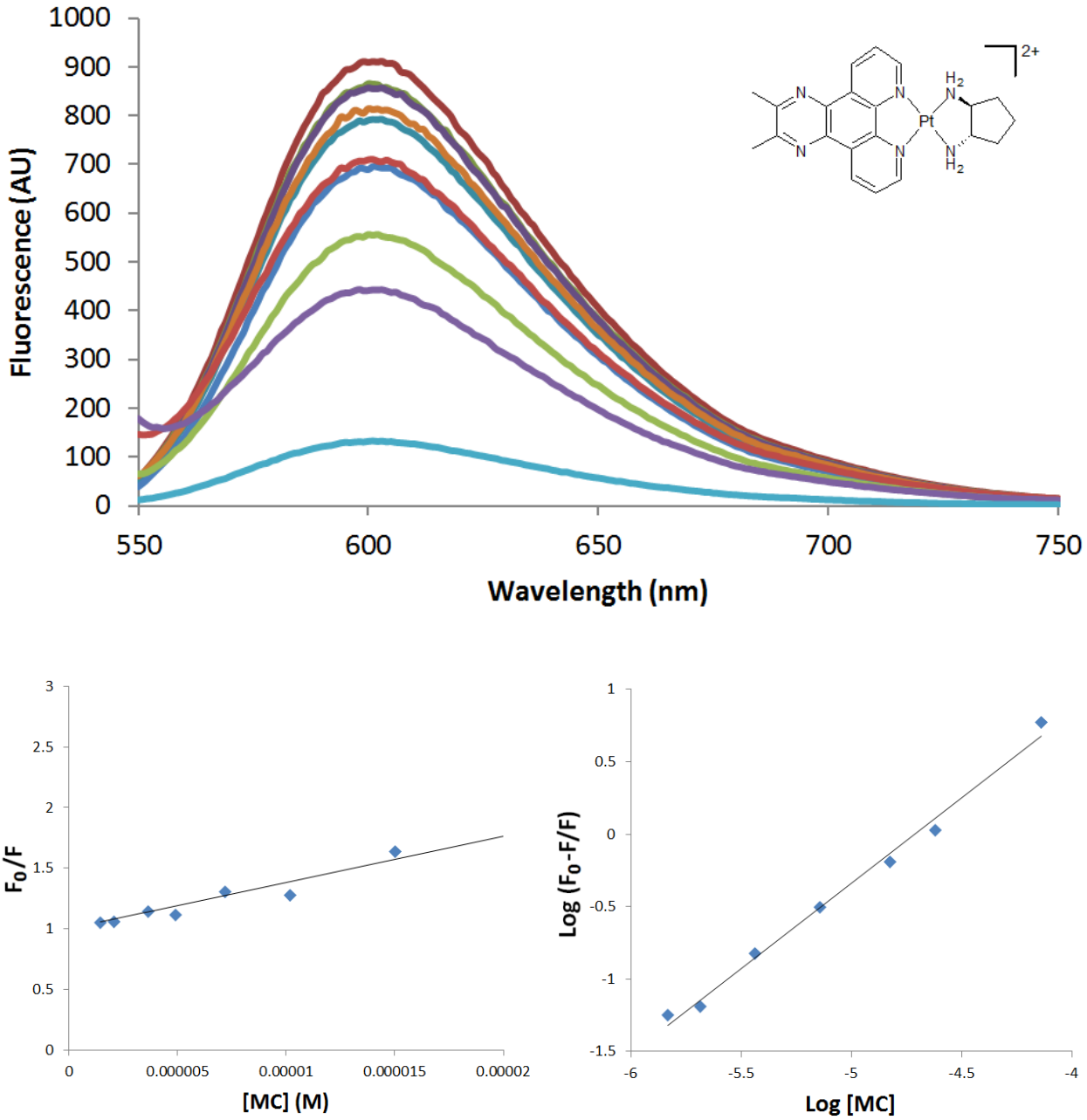

Figure S3.2.7. Fluorescence binding data for complex **7**, obtained from the first duplicate used: the emission spectra (top), Stern-Volmer plot (bottom left), and double-logarithm plot (bottom right).

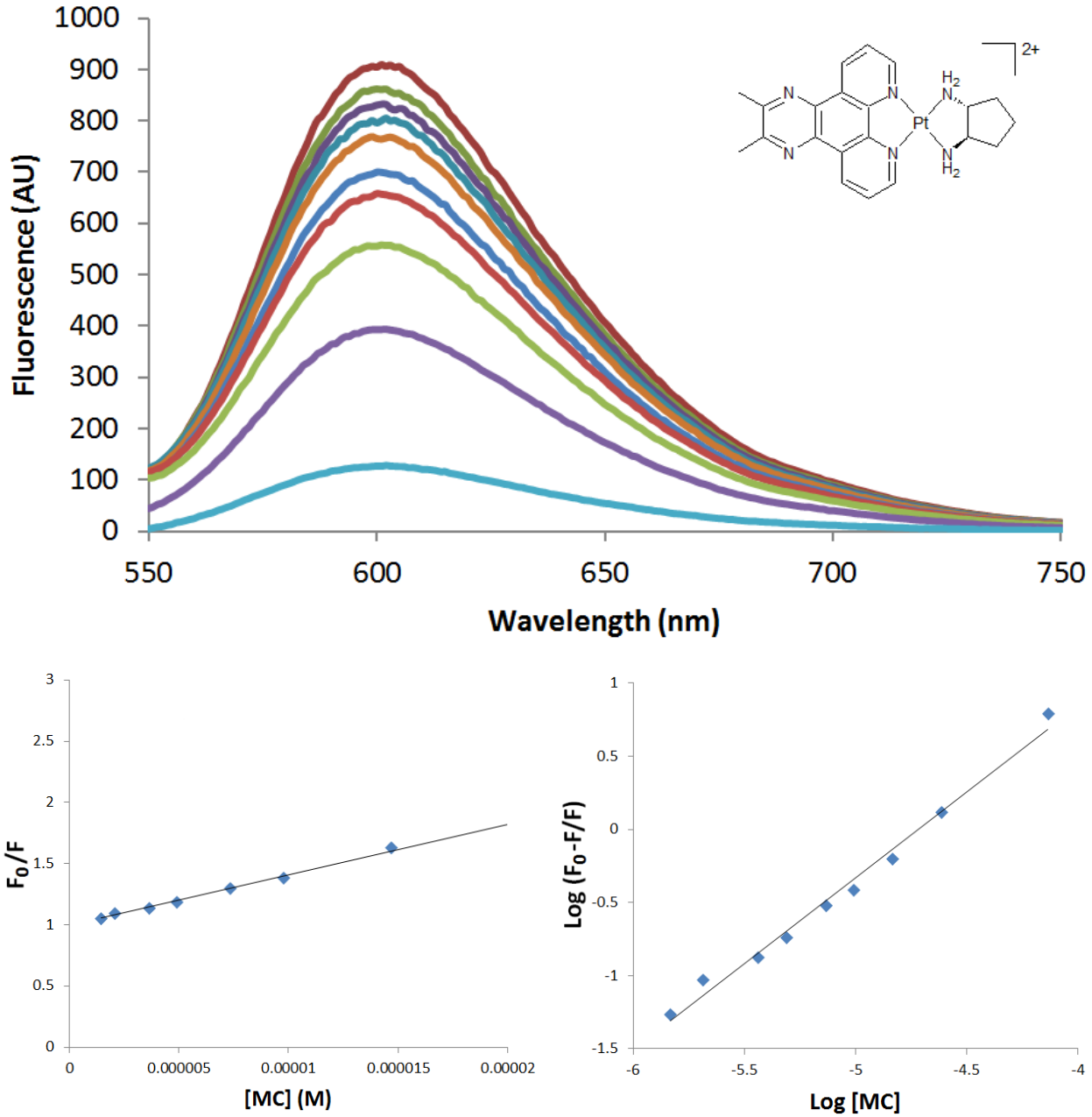

Figure S3.2.8. Fluorescence binding data for complex **8**, obtained from the first duplicate used: the emission spectra (top), Stern-Volmer plot (bottom left), and double-logarithm plot (bottom right).

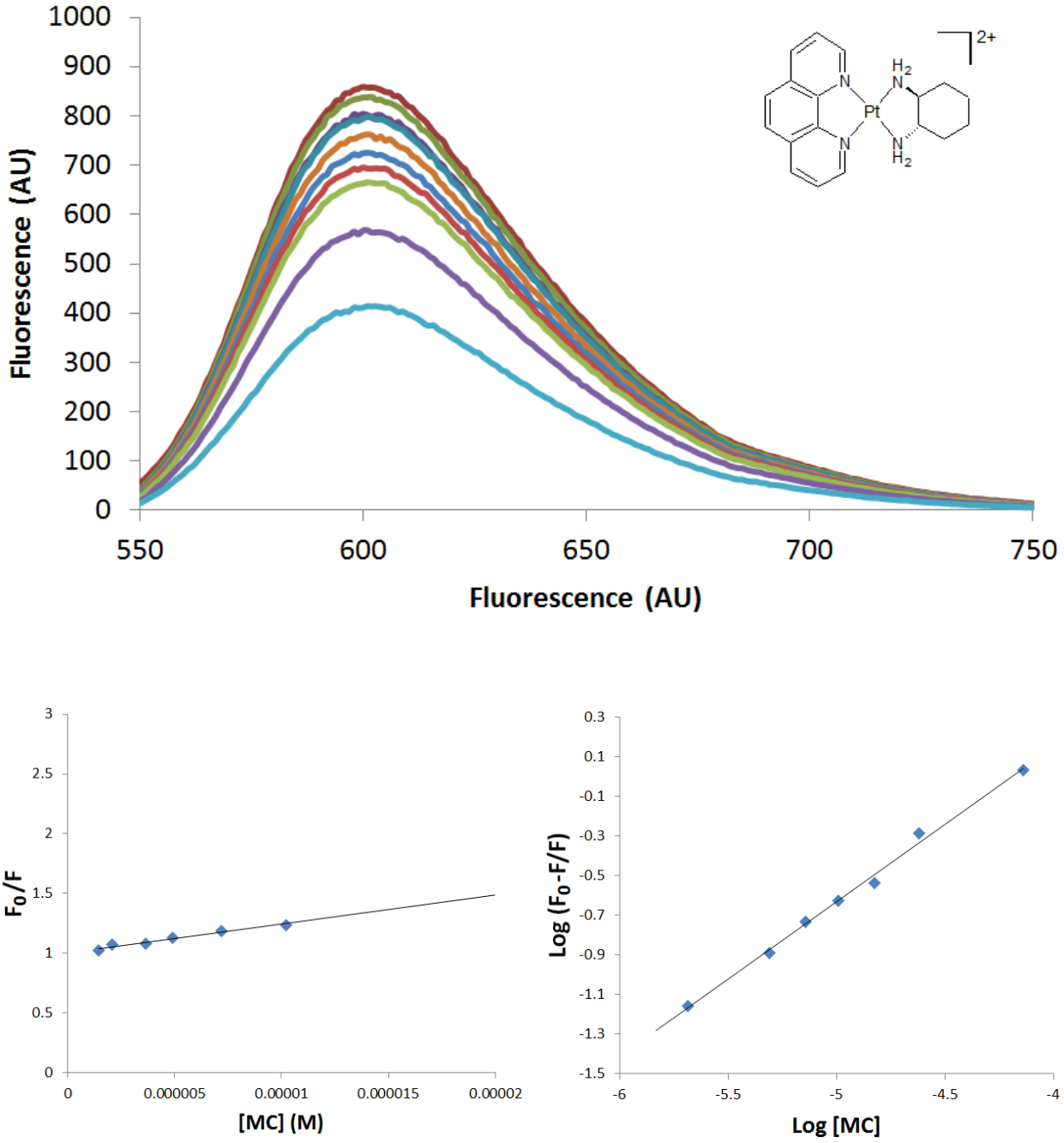

Figure S3.2.9. Fluorescence binding data for complex **9**, obtained from the first duplicate used: the emission spectra (top), Stern-Volmer plot (bottom left), and double-logarithm plot (bottom right).

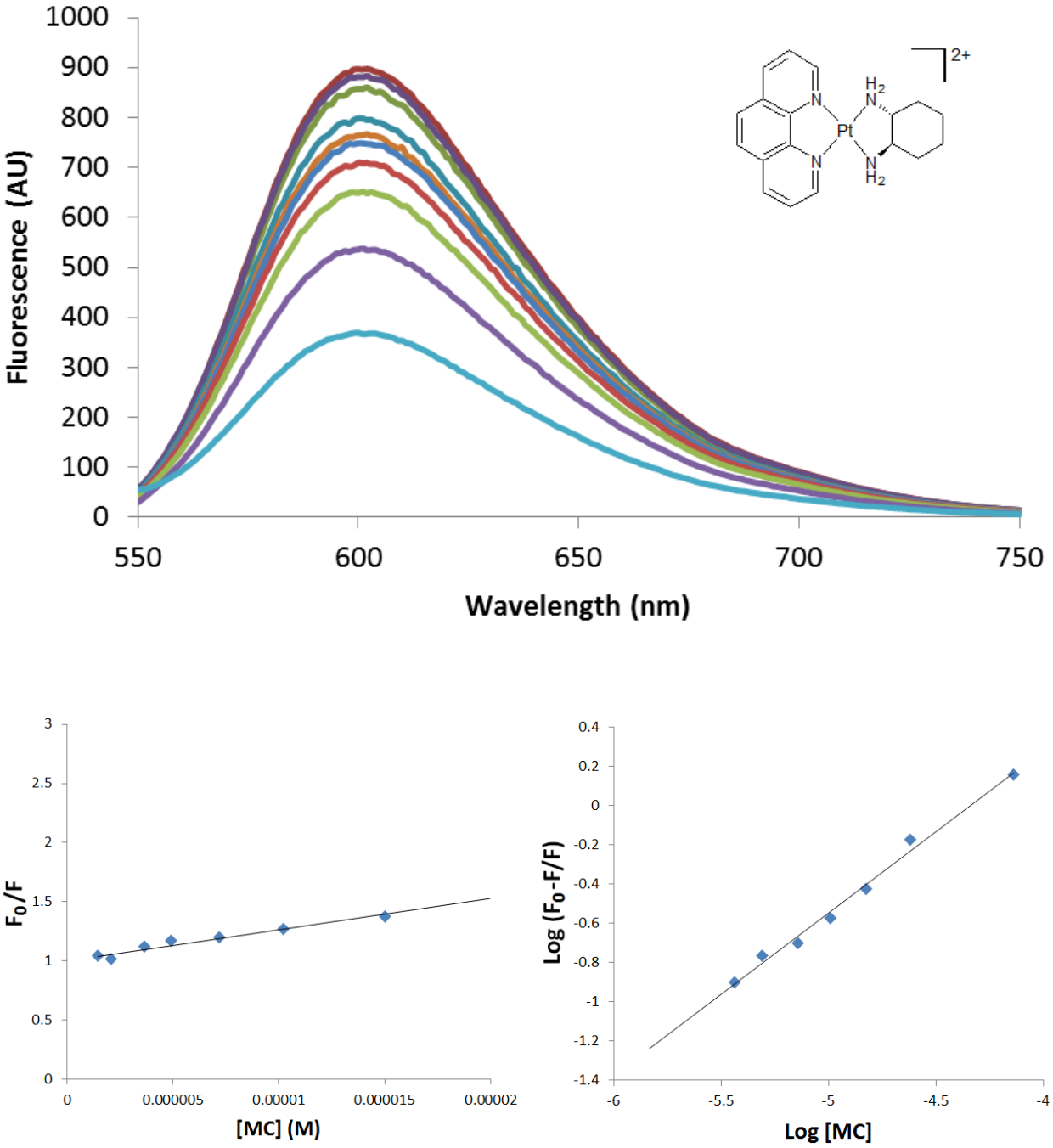

Figure S3.2.10. Fluorescence binding data for complex **10**, obtained from the first duplicate used: the emission spectra (top), Stern-Volmer plot (bottom left), and double-logarithm plot (bottom right).

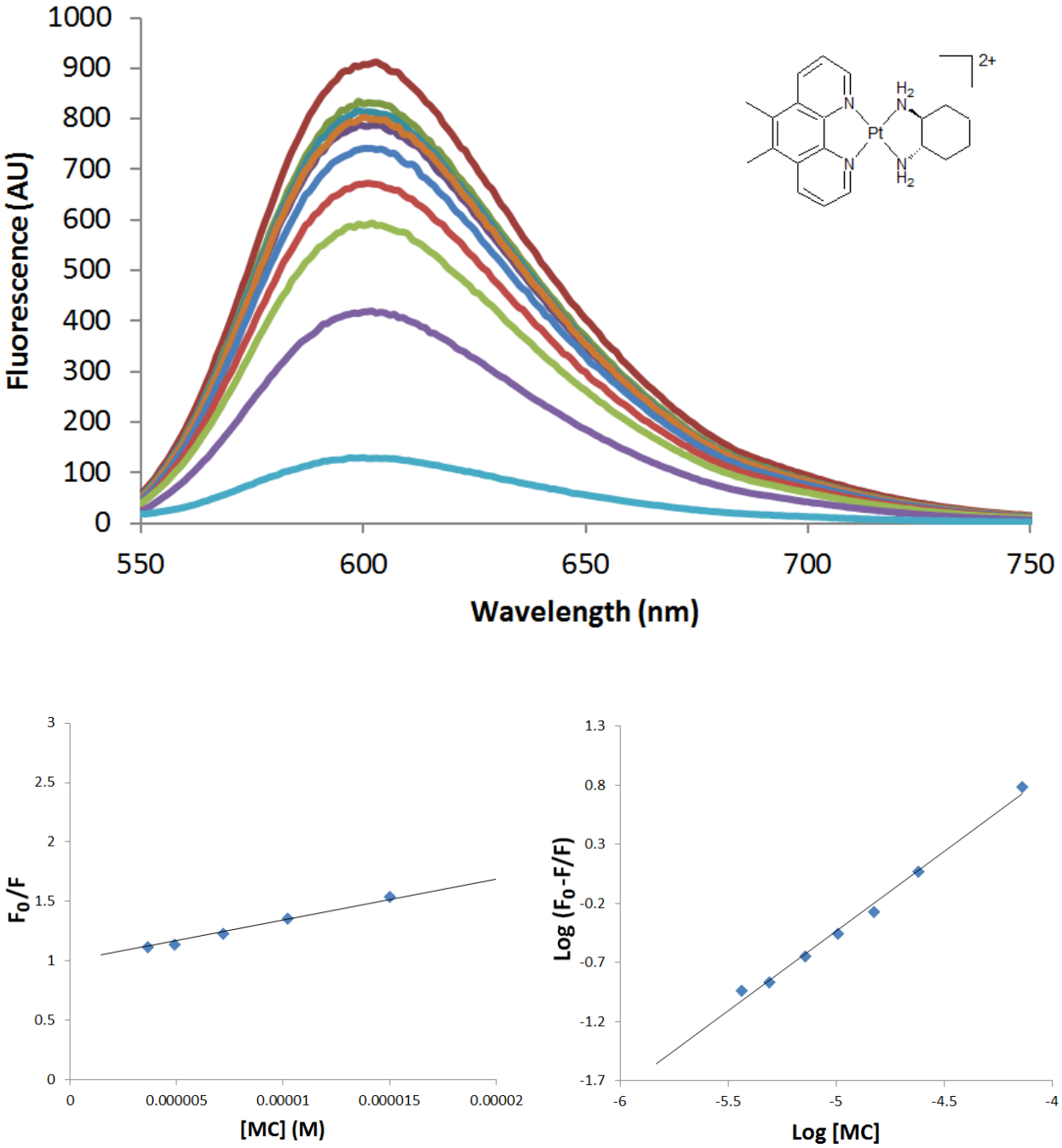

Figure S3.2.11. Fluorescence binding data for complex **11**, obtained from the first duplicate used: the emission spectra (top), Stern-Volmer plot (bottom left), and double-logarithm plot (bottom right).

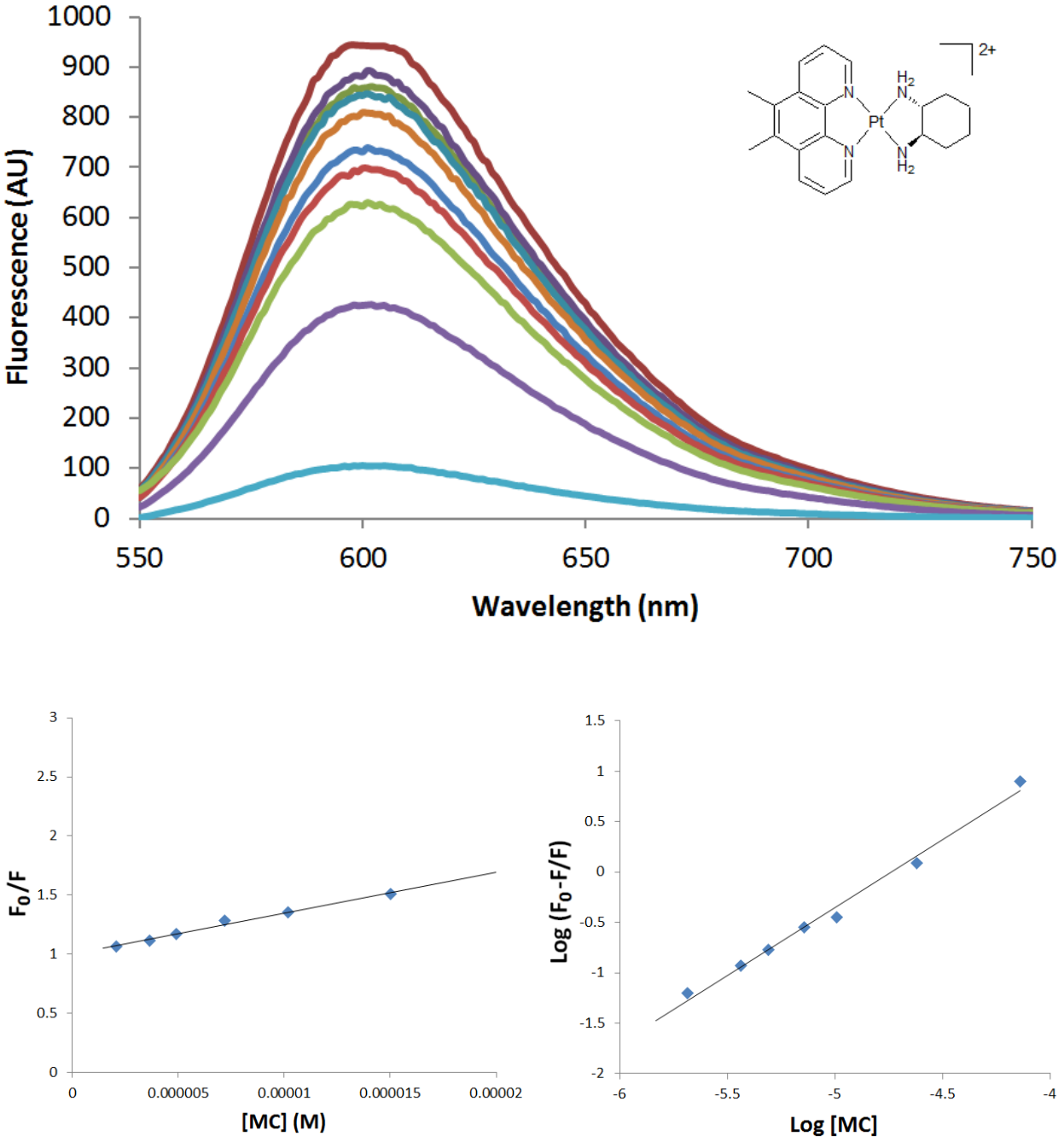

Figure S3.2.12. Fluorescence binding data for complex **12**, obtained from the first duplicate used: the emission spectra (top), Stern-Volmer plot (bottom left), and double-logarithm plot (bottom right).

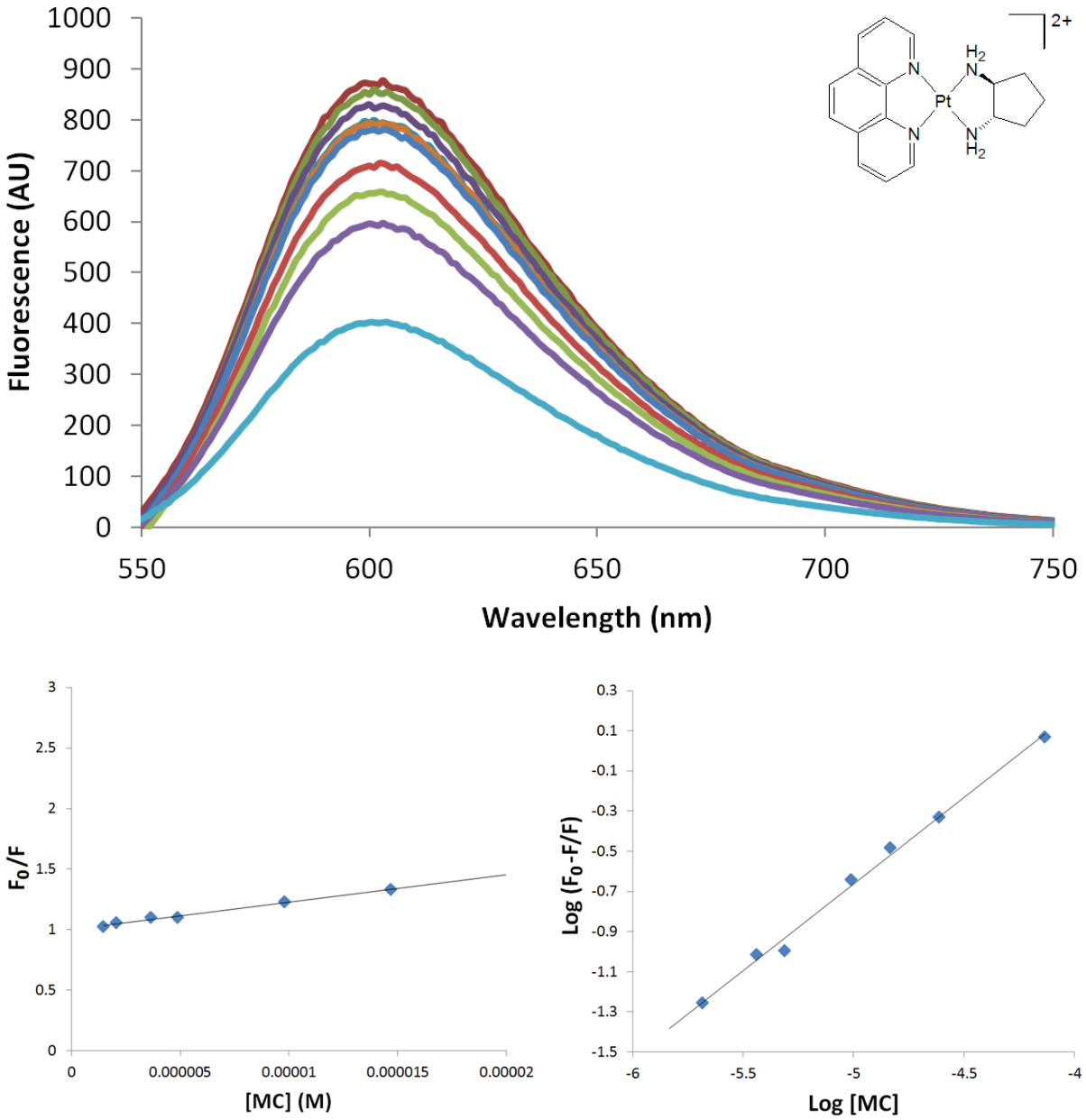

Figure S3.2.13. Fluorescence binding data for complex **13**, obtained from the first duplicate used: the emission spectra (top), Stern-Volmer plot (bottom left), and double-logarithm plot (bottom right).

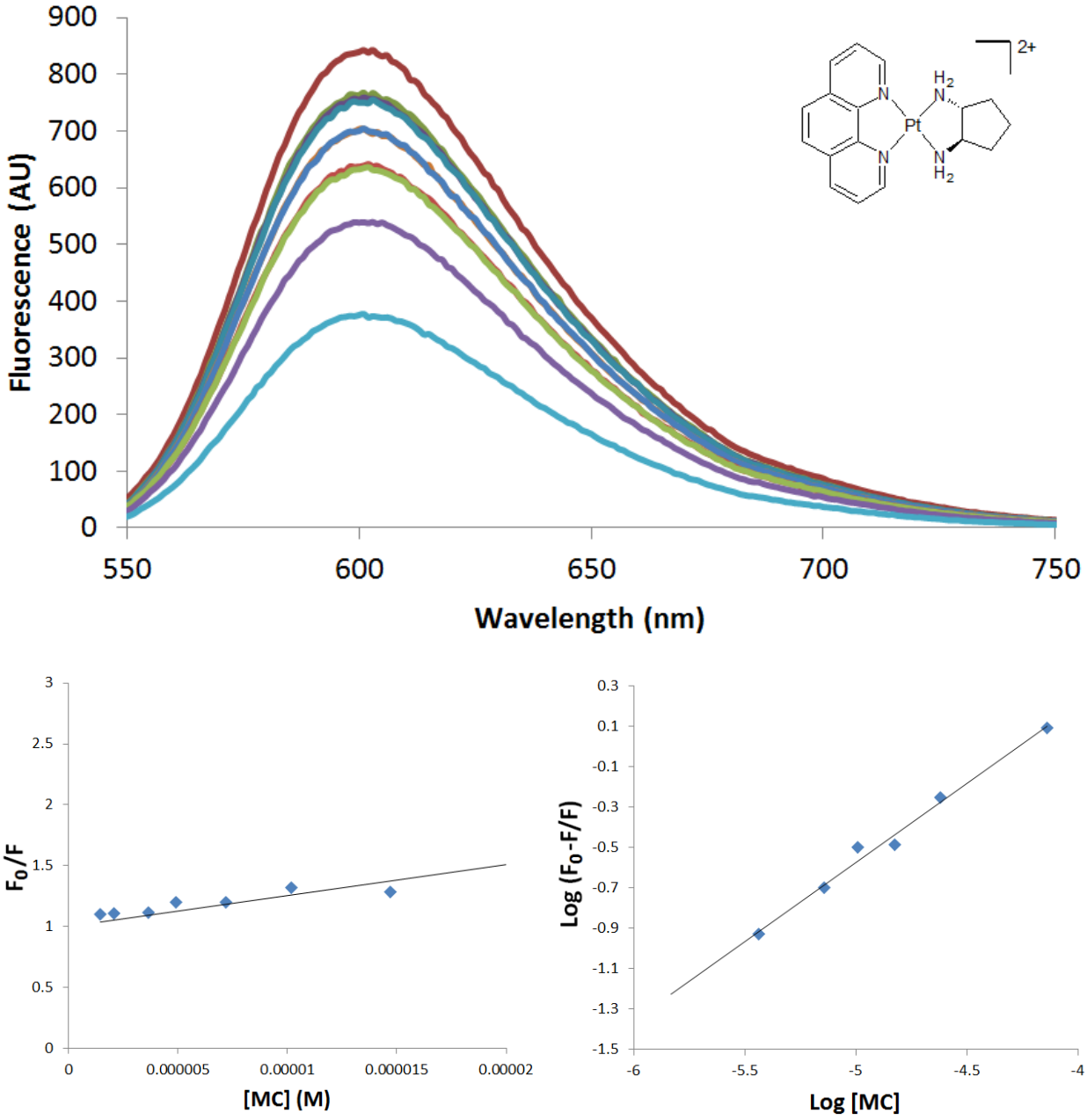

Figure S3.2.14. Fluorescence binding data for complex **14**, obtained from the first duplicate used: the emission spectra (top), Stern-Volmer plot (bottom left), and double-logarithm plot (bottom right).

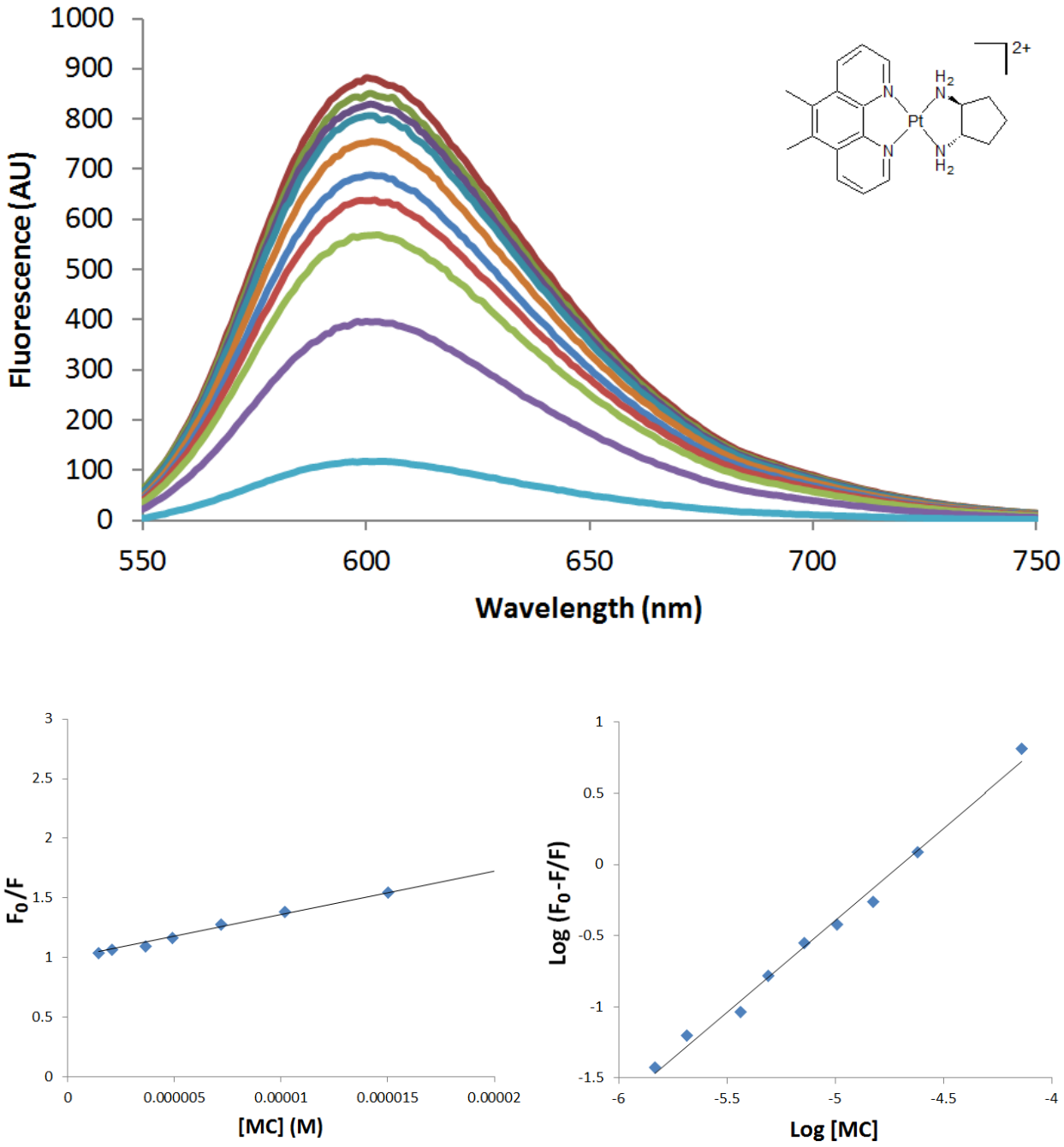

Figure S3.2.15. Fluorescence binding data for complex **15**, obtained from the first duplicate used: the emission spectra (top), Stern-Volmer plot (bottom left), and double-logarithm plot (bottom right).

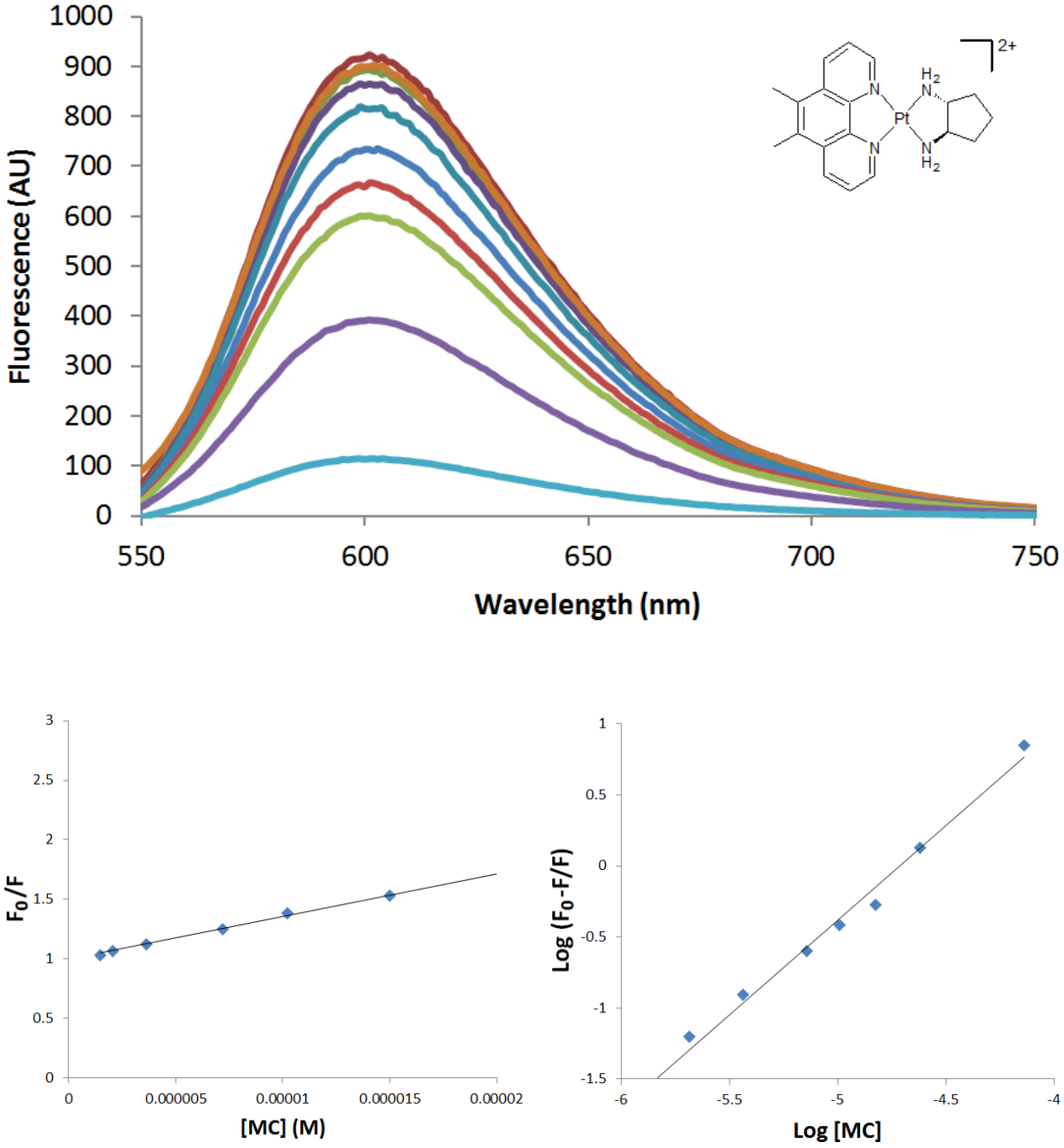

Figure S3.2.16. Fluorescence binding data for complex **16**, obtained from the first duplicate used: the emission spectra (top), Stern-Volmer plot (bottom left), and double-logarithm plot (bottom right).

S3.3. Stern-Volmer Data Summary

Table S3.3. Calculated K_q values for each PC in the FIDs. Standard error (±, one significant figure) is displayed.

Complex No.	Name	K_q / $M^{-1}.s^{-1}$ × 10^{12}	Complex No.	Name	K_q / $M^{-1}.s^{-1}$ × 10^{12}
1	DPQSSDACH	2.3 ± 0.6	**11**	PHENSSDACH	0.7± 0.3
2	DPQRRDACH	2.3 ± 0.4	**12**	PHENRRDACH	1.11 ± 0.04
3	23MEDSSDACH	2.3 ± 0.2	**13**	56MESSDACH	1.44 ± 0.06
4	23MEDRRDACH	2.1 ± 0.2	**14**	56MERRDACH	1.54 ± 0.03
5	DPQSSDACP	2.34 ± 0.06	**15**	PHENSSDACP	1.01 ± 0.02
6	DPQRRDACP	2.1 ± 0.9	**16**	PHENRRDACP	1.46 ± 0.06
7	23MEDSSDACP	1.74 ± 0.08	**17**	56MESSDACP	1.4 ± 0.2
8	23MEDRRDACP	1.82 ± 0.03	**18**	56MERRDACP	1.53 ± 0.03

References

1. Garbutcheon-Singh, K. B.; Leverett, P.; Myers, S.; Aldrich-Wright, J. R. Cytotoxic platinum(II) intercalators that incorporate 1*R*,2*R*-diaminocyclopentane. *Dalton Transactions* **2013,** 42, 918-926.
2. Harper, B. H.; Li, F.; Beard, R.; Garbutcheon-Singh, K. B.; Ng, N. S.; Aldrich-Wright, J. R. Biomolecular Interactions of Platinum Complexes. In *Supramolecular Systems in Biomedical Fields*, 1st ed.; Schneider, H. J., Ed. Royal Society of Chemistry: Cambridge, UK, 2013.
3. Wheate, N. J.; Taleb, R. I.; Krause-Heuer, A. M.; Cook, R. L.; Wang, S.; Higgins, V. J.; Aldrich-Wright, J. R. Novel platinum(II)-based anticancer complexes and molecular hosts as their drug delivery vehicles. *Dalton Transactions* **2007**, 5055-5064.